RGD-Modified Dendrimers for Drug Encapsulation and Targeted Inhibition of Tumor Cells

MASTER DISSERTATION

Xuedan He

MASTER IN NANOCHEMISTRY AND NANOMATERIALS

UNIVERSIDADE da MADEIRA

A Nossa Universidade

www.uma.pt

July | 2014

RGD-Modified Dendrimers for Drug Encapsulation and Targeted Inhibition of Tumor Cells

MASTER DISSERTATION

Xuedan He
MASTER IN NANOCHEMISTRY AND NANOMATERIALS

SUPERVISOR
Xiangyang Shi

CO-SUPERVISOR
Helena Maria Pires Gaspar Tomás

RGD-Modified Dendrimers for Drug Encapsulation and Targeted Inhibition of Tumor Cells

Thesis submitted to the University of Madeira in order to obtain the degree of Master in Nanochemistry and Nanomaterials

by Xuedan He

Study performed under the supervision of Prof. Xiangyang Shi and co-supervised by Prof. Helena Tomás

Centro de Competência de Ciências Exatas e de Engenharia,
Centro de Química da Madeira,
Campus Universitário da Penteada, 9000-390 Funchal, Portugal

Julho de 2014

DECLARATION

I hereby declare that this thesis is the result of my own work, is original and was written by me. I also declare that its reproduction and publication by Madeira University will not break any third party rights and that I have not previously (in its entirety or in part) submitted it elsewhere for obtaining any qualification or degree. Furthermore, I certify that all the sources of information used in the thesis were properly cited.

07/2014

ACKNOWLEDGEMENTS

I am grateful to everyone that directly or indirectly contributed to the execution of this work, especially to my supervisor Prof. Xiangyang Shi and to my co-supervisor Prof. Helena Tomás, for the collaboration and the guidance in my research and for providing the materials and facilities for the development of this project.

My gratitude to Dr. Carla Alves, not only for her guidance during all the work, but also for her friendship.

I want to thank Nilsa Oliveira, as whenever I needed to do nuclear magnetic resonance (NMR) spectroscopy, she always offered me help.

Special thanks to Prof. István Bányai and all the members in the Department of Colloid and Environmental Chemistry in the University of Debrecen.

I would like to thank also to all members of Centro de Química da Madeira (CQM), for the friendship and support, not only in the lab, but also in the meetings and gatherings.

I acknowledge the University of Madeira and CQM for providing me with the possibility to perform my master project.

Finally, I would like to acknowledge the Portuguese "Fundação para a Ciência e a Tecnologia" (FCT) for funding through the CQM Strategic Project PEst-OE/QUI/UI0674/2013, the NMR Portuguese Network PTNMR-2013, and the Projects PTDC/CTM-NAN/112428/2009 and PTDC/CTM-NAN/1748/2012. FCT and Santander Bank are also acknowledged for the Invited Chair in Nanotechnology of Prof. X. Shi.

During this master thesis, I learned chemical synthesis methods, and how to use several characterization devices such as the NMR spectrometer, the Ultraviolet-visible (UV-Vis) spectrometer, the Zetasizer, the Fluorescence Microscope, etc.. Moreover, I got acquainted with cell culture techniques (from recovering cells from liquid nitrogen to cytotoxicity tests of the modified dendrimers). In order to study the location of DOX in the dendrimer/DOX system, I got the chance to go to the Department of Colloid and Environmental Chemistry, Faculty of Science, University of Debrecen to do NMR research with Prof. István Bányai for around 2 months.

Work presentations in Scientific Meetings in the scope of the Master Project:

Xuedan He, Helena Tomás, Xiangyang Shi. RGD-modified dendrimers for drug encapsulation and targeted inhibition of tumor angiogenesis. Oral presentation in the 9th Materials Group Meeting of CQM. 31 January 2014; Funchal (Portugal).

ABSTRACT

In this study, cyclic arginine-glycine-aspartic acid (RGD) peptide-modified amine-terminated generation 5 poly(amidoamine) (G5.NH_2 PAMAM) dendrimers were prepared for the encapsulation of the anticancer drug doxorubicin (DOX) for targeted delivery to cancer cells overexpressing $\alpha_v\beta_3$ integrin cell surface receptors. First, the thiolated RGD peptide was linked to polyethylene glycol (PEG) *via* the bifunctional cross-linking reagent 6-maleimidohexanoic acid N-hydroxysuccinimide ester (MHS). Then a dendrimer modification process was performed in which the PEGylated RGD peptide and fluorescein isothiocyanate (FI) were covalently attached to the G5 dendrimers. This process was finally followed by acetylation of the remaining dendrimer terminal amines. The experimental results show that each G5.NHAc-FI-PEG-RGD dendrimer approximately encapsulated six DOX molecules. This formed complex is water soluble and stable. *In vitro* release studies proved that the multifunctional dendrimers facilitate a sustained release of DOX. More interesting, one-dimensional NMR and two-dimensional NMR were applied to investigate the interactions between dendrimers and DOX. Here, the impact of the environmental pH on the release rate of DOX from G5.NHAc-FI-PEG-RGD/DOX was fully studied. Furthermore, cell biological studies demonstrated that G5.NHAc-FI-PEG-RGD dendrimers have no cytotoxicity towards U87-MG cancer cells but that G5.NHAc-FI-PEG-RGD/DOX complexes have almost the same cytotoxicity as DOX alone. Moreover, due to the targeting ability of RGD, this dendrimer/drug system can also specifically target and display therapeutic efficacy to cancer cells overexpressing $\alpha_v\beta_3$ integrins. The cellular internalization of the multifunctionalized dendrimer was shown to be receptor mediated to an important extent. According to this study, we can say that G5.NHAc-FI-PEG-RGD is a promising system for the targeted therapy of different types of cancer.

Keywords: dendrimers; RGD peptide; doxorubicin; targeted cancer therapy.

RESUMO

Neste trabalho, foram preparados dendrímeros de poli(amidoamina) (PAMAM) de geração 5 (G5) funcionalizados com o péptido cíclico RGD para o encapsulamento do fármaco anticancerígeno doxorubicina (DOX) e sua entrega em células cancerígenas que expressem elevadas quantidades de integrinas $\alpha_v\beta_3$ na sua superfície (entrega específica do fármaco em células-alvo). No processo de síntese, o péptido contendo um grupo tiol foi primeiro ligado a uma cadeia de polietilenoglicol (PEG) através de um reagente de reticulação bi-funcional. De seguida, os dendrímeros foram ligados covalentemente ao péptido PEGilado e, ainda, ao isotiocianato de fluoresceína (FI), seguindo-se a acetilação (Ac) das aminas terminais remanescentes no dendrímero para se obter o sistema final G5.NHAc-FI-PEG-RGD. Os resultados experimentais mostram que, aproximadamente, existem 6 moléculas de DOX encapsuladas por G5.NHAc-FI-PEG-RGD, sendo estes complexos solúveis e estáveis em água. Os estudos *in vitro* mostraram que a libertação do fármaco a partir dos dendrímeros multifuncionalizados é controlada. O trabalho envolveu, ainda, estudos de NMR mono- e bi-dimensional na investigação da interacção existente entre os dendrímeros e as moléculas de DOX, e ainda a avaliação do impacto do pH ambiental na velocidade de libertação da DOX. Realizaram-se, igualmente, estudos biológicos com células U87-MG, os quais mostraram que os sistemas G5.NHAc-FI-PEG-RGD não apresentavam toxicidade e que, quando complexados com a DOX, apresentavam uma citotoxicidade semelhante à do fármaco usado de forma isolada.

Dada a afinidade do péptido RGD para as integrinas presentes em grande quantidade à superfície das células U87-MG, o sistema G5.NHAc-FI-PEG-RGD mostrou-se muito eficaz na entrega específica do fármaco e consequente eficácia terapêutica. A entrega do fármaco nas células mostrou ser, numa importante extensão, mediada pelos receptores (integrinas $\alpha_v\beta_3$) presentes à sua superfície. Este trabalho mostrou que os dendrímeros multifuncionalizados G5.NHAc-FI-PEG-RGD são

bastante promissores como sistemas para a entrega específica de fármacos em células cancerígenas.

Palavras chave: dendrímeros; péptidos RGD; doxorubicina; terapia do cancro dirigida

CONTENTS

LIST OF ACRONYMS

AA – Antibiotic and antimycotic

AML – Acute myelogenous leukemia

ASGPR – Asialoglycoprotein receptors

BBN – Bombesin

DAPI – 4',6-diamidino-2-phenylindole

DOSY – Diffusion-ordered spectroscopy

DOX – Doxorubicin

EDC – 1-ethyl-3-(3-dimethylaminopropyl)carbodiimide hydrochloride

EMEM – Eagle's Minimum Essential Medium

EPR – Enhance permeability and retention

FA – Folic acid

FI – Fluorescein isothiocyanate

FR – Folate receptor (FR)

GlcNAc – N-acetyl-D-glucosamine

GlcUA – D-glucuronic acid

Glut – L-Glutamine

GPI – Glycosylphosphatedylinositol

GRP – Gastrin-releasing peptide

HA – Hyaluronic acid

HPLC – High-performance liquid chromatography

MHS – 6-maleimidohexanoic acid N-hydroxysuccinimide ester

MMAE – Monomethylauristatin E

MTT – 3-(4,5-dimethyl-2-thiazolyl)-2,5-diphenyl-2-H-tetrazolium bromide

MTX – Methotrexate

NEAA – Non essential amino acids

NMR – Nuclear magnetic resonance

NOESY – Nuclear Overhauser enhancement spectroscopy

NPs – Nanoparticles

PAMAM – Poly(amidoamine)

PBS – Phosphate Buffered Saline

PEG – Polyethylene glycol

PLL – Poly(L-lysine)

PP – Primaquine phosphate

PPI – Polypropyleneimine

RGD – Arg-Gly-Asp

SP – Sodium pyruvate

TEA – Triethylamine

UV-Vis – Ultraviolet–visible spectroscopy

LIST OF FIGURES

LIST OF TABLES

CHAPTER 1 – INTRODUCTION

CHAPTER 1 – INTRODUCTION

1.1 Nanotechnology as a solution for drug delivery

In the last few years, the application of nanoparticles (NPs) in various disciplines and particularly in healthcare has been increasingly common, including but not limited to therapeutics (drug and gene delivery), diagnostics, and imaging (*1-4*). Among all of these applications, NPs as drug delivery vehicles are opening new opportunities for conventional drug formulations that present poor bioavailability or drug instability. The main advantages of using NPs as drug delivery systems are that they cannot only facilitate a controlled release of the drug (*5*) but also accumulate at the target sites, reducing the unwanted side effects of the therapeutic agents (*6*). There are several kinds of NPs that can serve as carriers for controlled drug delivery, such as ceramic NPs, metallic NPs, and polymer and dendrimer-based NPs (*7-10*).

1.2 Introduction of dendrimer

Dendrimers are polymeric molecules where the monomers are organized in branches that emanate radially from a central core (Figure 1) (*11*). The size of dendrimers is sufficiently small (e.g., the diameter of a generation 5 (G5) poly(amidoamine) (PAMAM) dendrimer is 5.4 nm (*12*)), which enables them to pass through the renal filter (*13*), eliminating the need for these molecules to be biodegradable. On the other hand, the surface of dendrimers can be easily modified with numerous functionalities, making them well suited as nano-scaffolds with desired targeting, imaging and therapeutic functions (*14-16*). Furthermore, the internal cavities of dendrimers can be used for host-guest interactions and encapsulation of guest molecules (*1, 17-20*). In addition, the terminal groups of dendrimers can also be modulated to avoid issues of toxicity and nonspecific cell

membrane binding. For example, acetylation (*21-24*), hydroxylation (*25*) or carboxylation (*26*) of dendrimers possessing amine termini can significantly improve the biocompatibility of dendrimers. Polyethylene glycol (PEG), which behaves as a linker and which is considered as the gold standard for stealth polymers in the emerging field of polymer-based drug delivery, may also be considered when modifying dendrimers. In fact, full or partial PEGylation of dendrimers effectively increases the blood stream circulation time of these molecules as well as increases their biocompatibility (*27-29*).

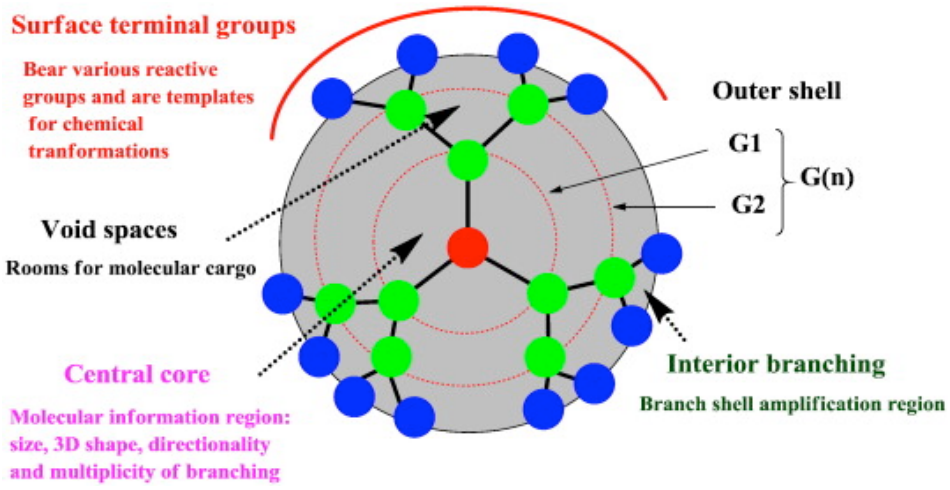

Figure 1 – 2D schematic illustration of a dendrimer. Taken from ref. (*30*) .

The synthesis used for dendrimer preparation permits an almost entire control over critical molecular design parameters such as size, shape, surface/interior chemistry, flexibility, and topology. As is shown in Figure 2, in principle, there are two ways for the synthesis of dendrimers. "A divergent method", in which the synthesis begins from a polyfunctional core and continues radially outwards by successive stepwise activation and condensation. Dendrimers can also be prepared using a convergent method, where preformed branched dendritic polymers connect to each other via a central core-mediated reaction (*31*).

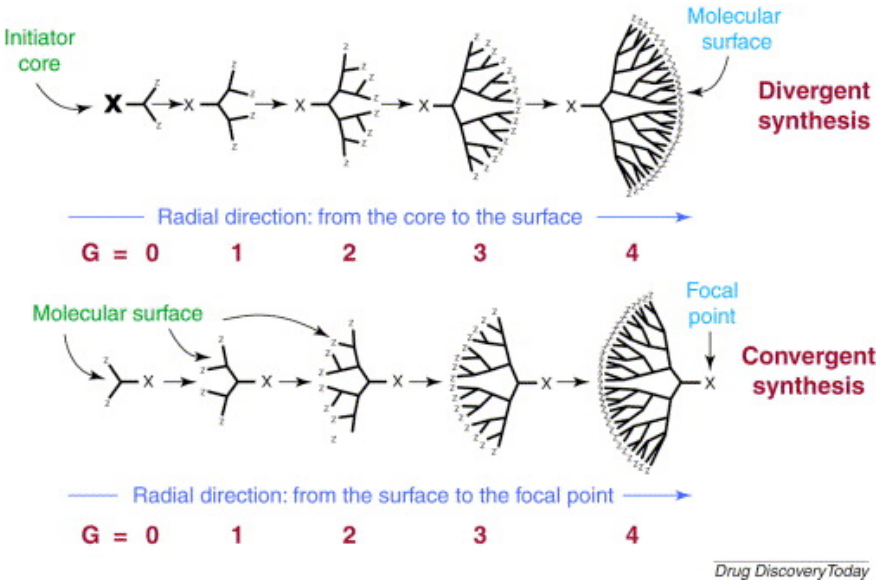

Figure 2 – Two principle synthetic methods for constructing dendritic macromolecules (dendrons): (a) the divergent method and (b) the convergent method. Taken from ref. (*31*).

Among all the dendrimers, the most commonly referenced dendrimers used in nanomedicine are based on PAMAM (Figure 3), poly(L-lysine) (PLL), polyesters, polypropyleneimine (PPI) and poly(2,2-bis (hydroxymethyl) propionic acid) (*30*). In conclusion, the well-defined structure, compact globular shape, mono-dispersed size, and controllable surface functionalities of dendrimers make them versatile platforms for drug delivery applications.

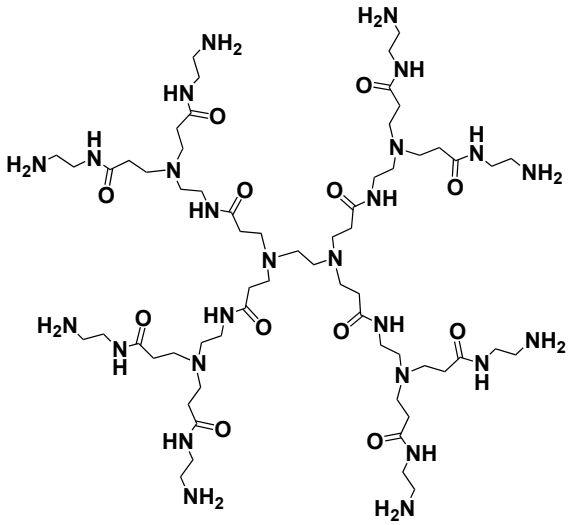

Figure 3 – Structure of a PAMAM dendrimer (Starburst^{TM}).

1.3 Dendrimer – based drug delivery systems

Doxorubicin (DOX) (structure see Figure 30) is a cancer drug widely used in the treatment of hematological malignancies, many types of carcinoma, and soft tissue sarcomas (*32-34*). Similar to other conventional anticancer drugs, free DOX is water-insoluble, cytotoxic to normal cells or tissues and easy to be cleared by the blood stream (*20*), limiting its clinical applications. As a consequence, it may be advantageous to use dendrimers as carriers for free DOX (*35*).

DOX can be loaded on dendrimers either through physical encapsulation/complexation or covalent linkage (Figure 4) (*20, 36*). Both of these two methods have their own advantages and drawbacks.

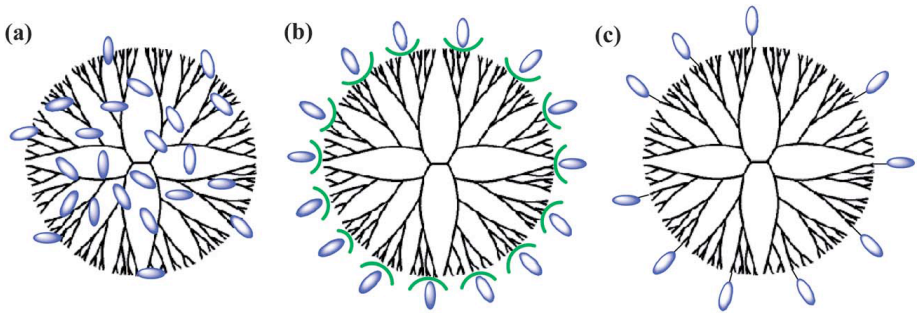

Figure 4 – Dendrimer drug delivery systems of different types (the blue color represents the drug agents). Drugs can be physically entrapped inside the dendrimer (a), adsorbed on the surface of the dendrimer through intermolecular interaction forces (b), or be conjugated to the dendrimer (c). Taken from ref. (*37*).

1.3.1 DENDRIMER/DRUG COMPLEXES

Both hydrophobic and hydrophilic drugs can be carried by dendrimers. The hydrophobic drugs can be easily encapsulated inside the hydrophobic internal "cavities" of an appropriately designed dendrimer (*18*). For hydrophilic drugs, they can be complexed with the dendrimer surface groups through hydrogen bonding, *van*

der Waals interactions, and electrostatic interactions (*38*). Sustained release of encapsulated molecules can be achieved on the basis of the size, shape and surface charge of the dendrimer and even through finely tuned hydrolytic conditions for partial or complete removal of the dendrimer shell (*37, 39*).

In comparison with a dendrimer/drug conjugate, the formation of a dendrimer/drug complex is much more simple and straightforward, and is normally done by just mixing the dendrimers and the drugs in either an aqueous solution or in a mixture of solvents. The chemical structure of the drug to be loaded remains unchanged after the complexation process, which ensures the therapeutic efficacy of the drug. However, it is usually difficult to control the loading capacity and the release profile of the drugs because the loading of the drug is based on physical interactions between the drug and the dendrimer. In the study of Wang *et al.* (*1, 20*), they modified acetylated G5 PAMAM dendrimer with fluorescein isothiocyanate (FI) and folic acid (FA), then used this modified dendrimer to encapsulate drugs. They found that approximately one DOX molecule could be encapsulated within each G5.NHAc-FI-FA dendrimer, and that 3.7 molecules of 2-methoxyestradiol could be encapsulated into each G5.NHAc-FI-FA using the same molar ratio of dendrimers and drugs. They hypothesized that the higher encapsulation efficiency of 2-methoxyestadiol compared to that of DOX might be due to the smaller molecular size of 2-methoxyestadiol (Mw = 302.4 g/mol) relative to that of DOX (Mw = 543.5 g/mol). The small size of 2-methoxyestadiol in the dendrimer-based scaffold thus accounts for a higher encapsulation efficiency; in contrast, the larger size of DOX in the dendrimer-base scaffold will limit its entrance and retention within the dendrimer interior.

1.3.2 DENDRIMER/DRUG CONJUGATES

Dendrimer/drug conjugates are obtained when the chemotherapeutic drugs are covalently attached to the peripheral groups of the dendrimer. Conjugation generally requires multi-step organic reactions, leading to a low yield of the final conjugate.

Also, in most of the cases, the covalent conjugation chemistry has to be optimized in order to get cleavable bonds and allow the release of the drug molecules under specific biological conditions. However, there is an extremely useful advantage of dendrimer/drug conjugates related with the fact that the covalent linkage between dendrimers and drugs is stable *in vivo*, providing a better control over drug release. Until now, numerous chemotherapeutic drugs have been conjugated onto the surface of dendrimers through amide, ester, hydrazone, imine, disulfide, carbamate, and enzyme-cleavable peptide sequence bonds (*35, 40-42*). Each linkage system has its own cleavage mechanism to separate the drug molecules from the dendrimers such as reactions promoted by endogenous physiological factors like the redox potential, pH, and the presence of hydrolytic enzymes (Figure 5) (*41, 43*). In a recent study, Choi *et al.* (*44*) reported the light-controlled release of caged DOX from folate receptor (FR)-targeting PAMAM dendrimer nanoconjugates. They attached DOX through a photocleavable linkage to a FA-attached G5 PAMAM dendrimer. *In vitro* studies showed that the drug release from this conjugate was controllable, and highly dependent on UV light exposure time.

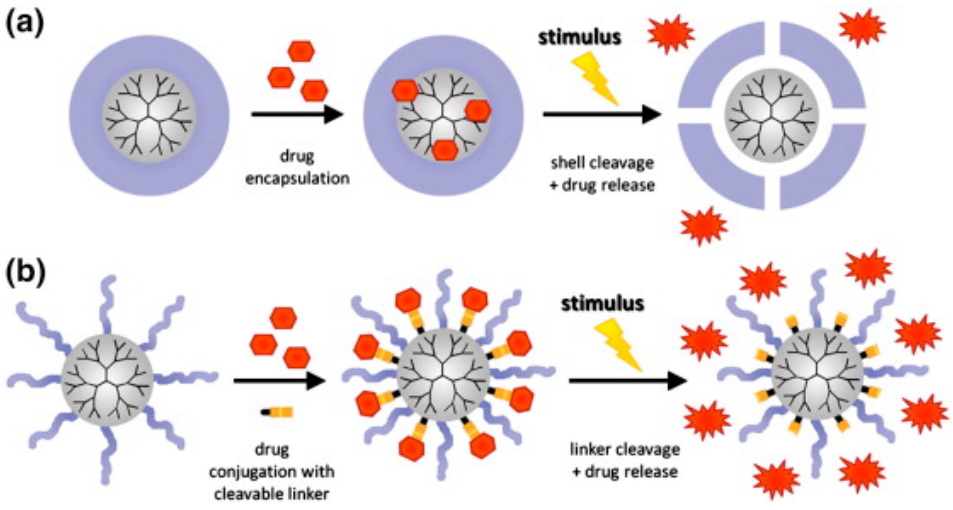

Figure 5 – Different mechanisms for stimuli-responsive release of active agents from nanocarriers: (a) supramolecular complexes like dendritic core-shell particles with a cleavable shell and (b) dendritic scaffolds with attached solubilizing/stealth groups using cleavable linkers for the drug conjugation. Adapted from ref. (*42*).

1.4 Targeted drug delivery

Several drugs have been discovered that exhibit anticancer properties. Unfortunately, most of them have undesirable toxicity towards normal tissues, i.e., they do not target only cancer cells, or they do not interfere only with the metabolic pathways of cancer cells. Nowadays, researchers have begun to focus on decreasing the side effects associated with drugs, as well as discovering drugs with improved delivery ability to tumor tissue in man. This goal should lead to an improved quality of life and an increased life expectancy for the patients.

There are several methods that have been studied to direct drugs to the target tumors. In general, two different approaches can be used: passive and active. The action mechanism of passive targeting drug delivery systems is based on the anatomical characteristics of the tumor tissue and is referred to as the "enhanced permeability and retention" (EPR) effect. In this phenomenon, there is an accumulation of the delivery systems that transport the drug into the tumor (solid tumor) as a consequence of an increased permeability of the immature blood vessels that were formed in the tumor interior and the absence of lymphatic drainage (*45*). With EPR targeting, drugs are released locally and taken up by tumor cells subsequently. In contrast, active targeting can be achieved using specific interactions between receptors on the cell surface and exposed targeting moieties in the drug delivery system (*46*). In this approach, a vehicle can be used to carry a therapeutic or a bioactive agent such that this agent directly binds to the target site for selective delivery. Therefore, the active approach takes advantage of the EPR effect but further increases selectivity through receptor-mediated uptake by target cancer cells. In this case, to further improve their efficiency, drug carriers can be modified with different types of targeting agents (*47*). For example, the literature reports the functionalization of dendrimers with FA (*46*), hyaluronic acid (HA) (*48*), monoclonal antibodies (*49*), and peptides (*50, 51*) before drug loading.

1.4.1 FA TARGETED DELIVERY SYSTEMS

The FR is a glycosylphosphatidylinositol (GPI)-linked membrane glycoprotein that has folate affinity, normally with an apparent molecular weight of 38–40 kDa (*52*). It is reported that FR is expressed or overexpressed in many types of tumors, including ovarian (52 of 56 cases tested), endometrial (10 of 11 cases tested), colorectal (6 of 27 cases tested), breast (11 of 53 cases tested), lung (6 of 18 cases tested) and kidney (9 of 18 cases tested) tumors, as well as brain metastases derived from epithelial cancers (4 of 5 cases tested) and neuroendocrine carcinomas (3 of 21 cases tested) (*53*). However, the receptor is generally absent in most healthy tissues with the exceptions of the choroid plexus and the placenta, and low receptor levels are detected in the lung, thyroid and kidney (*54*). The general model for the cellular uptake of drug conjugates or complexes targeted to the FR is illustrated in Figure 6. The high concentration of FR on the surface of tumor cells makes it a good agent for targeted drug delivery to the mentioned tumors. In this respect, Hong *et al.* (*55*) have demonstrated that 5-6 FA per G5 PAMAM dendrimer achieved saturated binding affinity.

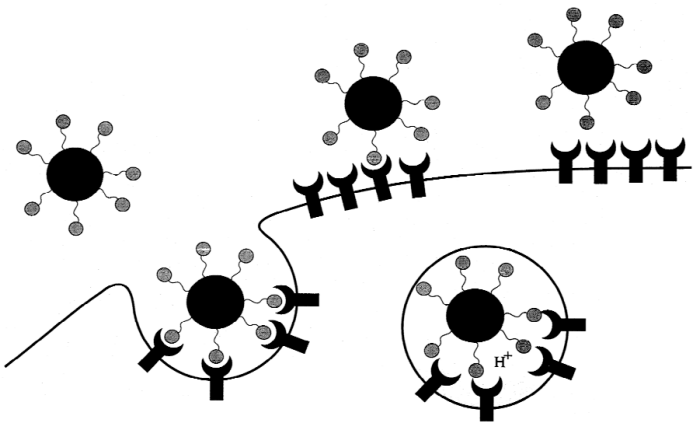

Figure 6 – A schematic diagram of the FR-mediated endocytosis pathway. Adapted from ref. (*56*).

The FA-mediated targeting enables both dendrimer/drug conjugates and dendrimer/drug complexes to specifically inhibit the growth of tumor cells. A study of Patri *et al.* (*46*) used G5 PAMAM dendrimers as a platform to covalently link FA (G5-FA), followed by complexation or conjugation with the anticancer drug methotrexate (MTX). In *in vitro* biological experiments using the same concentration of MTX, cell viability was much lower when the system G5-FA/MTX was applied to KB cells overexpressing the FA receptor (FAR positive cells, FAR+) (Figure 7) when compared to KB cells with FA pre-blocked FAR (Figure 8). Moreover, the results also showed that a cleavable, covalently linked dendrimer conjugate performed better targeting drug delivery, as it does not release the drug prematurely in biological conditions (Figure 9).

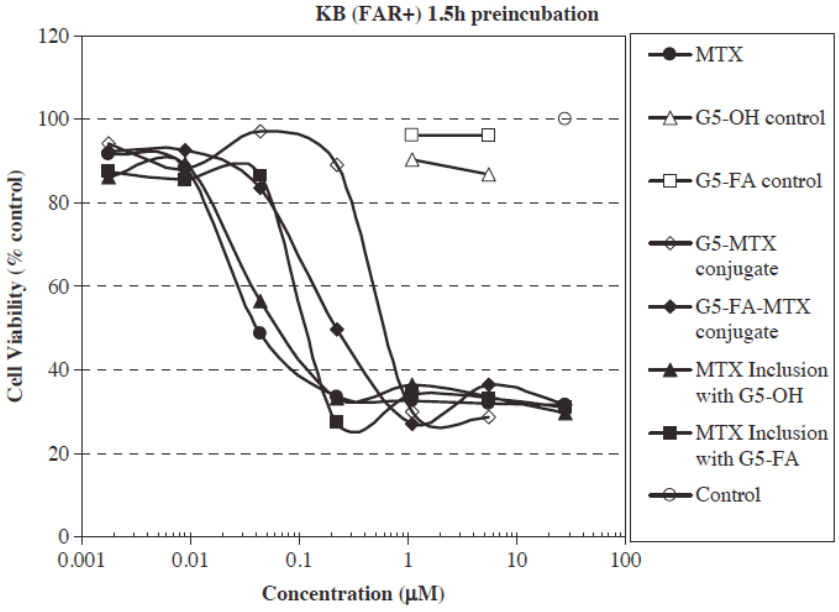

Figure 7 – Cytotoxicity of covalent conjugates with MTX and dendrimer inclusion complexes with MTX tested on KB cells over-expressing the FA receptor (FAR+). Cells were pre-incubated for 1.5 h with MTX containing dendrimers, and dendrimers without drug, washed with medium and further incubated for 72 h. Adapted from ref. (*46*).

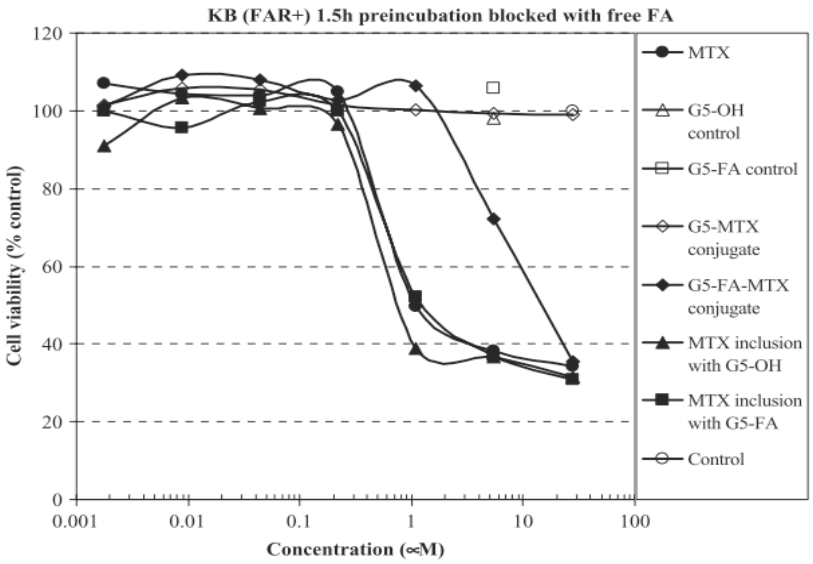

Figure 8 – Specificity of delivering FA-targeted MTX conjugates and inclusion complexes. Cytotoxicity was tested using KB (FAR+) cells after initial blocking with cell culture with free FA (9 μM) followed by pre-incubation with compounds for 1.5 h, wash and further incubation for 72 h. Adapted from ref. (*46*).

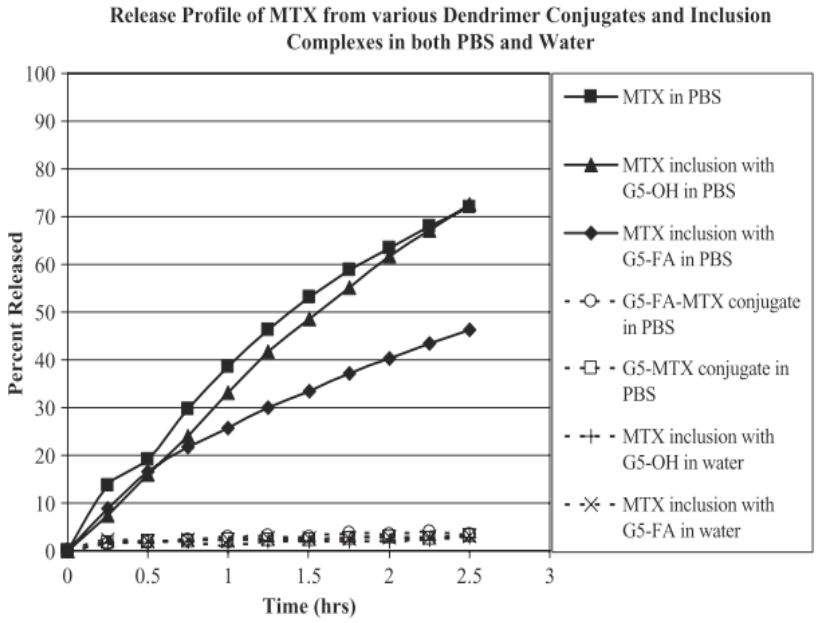

Figure 9 – Comparative release profile of MTX from inclusion complexes and conjugates in water and phosphate-buffered saline (PBS). Adapted from ref. (*46*)

1.4.2 HYALURONIC ACID TARGETED DELIVERY SYSTEMS

Hyaluronic acid (HA) is a linear polysaccharide of alternating D-glucuronic acid (GlcUA) and N-acetyl-D-glucosamine (GlcNAc) units (see Figure 10). It is the only non-sulfated glycosaminoglycan and it occurs primarily *in vivo* as sodium hyaluronate. HA can be found present in the extracellular matrix (e.g., in cartilage), and in the synovial fluid of joints. It is an immunoneutral building block that can be used for preparing biocompatible and biodegradable biomaterials, and has been employed as both a vehicle and an angiostatic agent in cancer therapy (*57*).

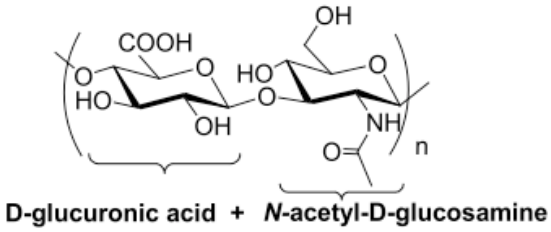

Figure 10 – Structure of HA. Adapted from ref. (*47*).

HA serves a variety of functions within the extracellular matrix. One of its most important functions is that it can direct receptor-mediated effects on cells. These effects occur through the activation of intracellular signaling pathways inside cells. Numerous cell-membrane-localized receptors (HA binding proteins) have been identified, such as CD44, RHAMM, IVd4, and the liver endothelial cell clearance receptor (*58-60*), among which the CD44 receptors on tumor surfaces have been well studied. Moreover, HA acts as a signaling molecule in cell motility, inflammation, wound healing, and cancer metastasis (*61*).

The targeting principle of HA is that most malignant solid tumors contain elevated levels of HA compared to healthy cells. Because of poor differentiation and a lower survival rate of some human carcinomas, the level of HA in malignant solid tumors becomes higher, providing a matrix that facilitates invasion. In general, HA internalization is matrix receptor mediated. Receptors including CD44, can mediate cell-matrix interactions, giving information to the cells but also giving feedback to the

matrix (*57*)**.** So HA is a promising targeting agent that we can use to conjugate to the drug carrier system. Low molecular weight HA has been reported to be directly conjugated to cancer drugs such as butyric acid (*62*), paclitaxel (*63*), and DOX (*64*). These studies proved that HA bearing polymers can be a suitable non-toxic drug carrier. These polymer/drug systems can be quickly internalized into cancer cells, and release the drug in a sustained manner restoring the original cytotoxicity of drugs.

The advantages of HA as a targeting agent are not limited to the above description. HA production is quite biocompatible, which to a large extent facilitates the synthesis and design of HA and drug bearing bioconjugates. Moreover, HA is hydrophilic, which allows its manipulation and application in aqueous media. However, a possible disadvantage of HA is the lack of accurate structural characterization of the conjugates (*47*).

1.4.3 MONOCLONAL ANTIBODY TARGETED DELIVERY SYSTEMS

As we can see in Figure 11, the general structure of antibodies (150kDa) consist of two heavy chains (50kDa each) and two light chains (25kDa each) that are linked by disulfide bonds (*47*). The principle of antibody – targeted delivery systems is that there are specific antigens overexpressed or expressed on the surface of cancer cells, and so selective antibodies can be conjugated with cytotoxic drugs or drug delivery systems (*65, 66*). These conjugates can be internalized via receptor – mediated endocytosis and then active drugs can be released into the target sites without a decrease in their original activity. The use of antibodies as targeting agents has a long story. In 2000, the Food and Drug Administration (FDA) approved Mylotarg® (gemtuzumab-ozogamicin) to be utilized in the clinic as an antibody-drug immunoconjugate for the treatment of acute myelogenous leukemia (AML) (*67*).

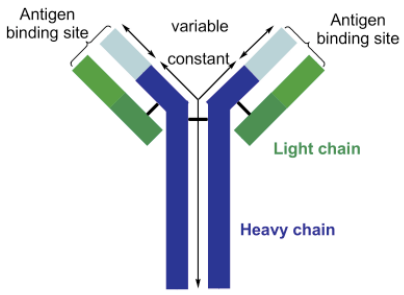

Figure 11 – Structure of an antibody. Adapted from ref. (*47*).

According to the different kinds of antigens overexpressed on tumor cell surfaces, there are different kinds of drugs that can be used in the immunoconjugates, such as calicheamicin (*67*), maytansine derivative DM1 (*68*), CC-1065 (*69*), monomethylauristatin E (MMAE) (*70*), DOX (*71*) and a second-generation taxoid (*65*). In addition, there are also different sorts of linker moieties between antibodies and drugs that can be chosen, including the hydrazine (*72*), peptide (*73*), and disulfide (*65*) linkers. In order to achieve the highest efficacy of the immunoconjugates, it is critically important to choose a linker that is stable when in circulation in the body and that can be efficiently cleaved inside the cancer cells. The three mentioned linkers are the most common and have their own advantages and disadvantages. For instance, the hydrazone linker is good to use under acidic conditions in lysosomes (about pH 5) to release the cytotoxic drug via non-enzymatic hydrolysis, but it is unstable during circulation. Peptide linkers are specifically designed for rapid lysosomal hydrolysis. Disulfide linkers can be easily cleaved inside the tumor cells via disulfide exchange (reduction reaction) (*47*).

However, it is important to take into consideration the molecular weight of the antibody-drug conjugates, since a high molecular weight is good in terms of the EPR effect, but a big size often leads to poor penetration into tumor cells. Researchers found some methods to truncate antibody fragments in order to achieve a faster penetration into tumors, but unfortunately, the circulation time was shortened by renal clearance (*74*). Another problem related with the antibody containing drug delivery systems is that there is a limited number of molecules that can be loaded without

decreasing the binding affinity of the antibody targeting moiety (*66*).

1.4.4 GLYCOSYLATED DENDRIMER-BASED TARGETED DELIVERY SYSTEMS

The term 'glycodendrimer' has been used to describe a wide range of dendrimer architectures that incorporate carbohydrates into their structure. It is well known that asialoglycoprotein receptors (ASGPR) are present on the surface of hepatocytes and several human carcinoma cell lines with a high density, showing a strong binding affinity with galactose. Therefore, dendrimers have been glycoconjugated for targeting human liver cancer cells overexpressing the ASGPR (*75*). In general, there are three kinds of glycodendrimers: carbohydrate coated, carbohydrate-centered and carbohydrate-based types. Bhadra *et al.* (*76*) reported the use of galactose-coated PPI dendrimers for targeted delivery of the antimalarial drug primaquine phosphate (PP) to the liver. The results revealed that galactose coating of PPI dendrimers has higher drug entrapment efficiency, longer drug release time and higher hepatic accumulation of PP compared with non-functionalized PPI dendrimer formulations.

1.4.5 PEPTIDE TARGETED DELIVERY SYSTEMS

There are several tumor-associated receptors for peptides. Nowadays, peptide targeted delivery systems are becoming more and more attractive because the needed sequences of amino acids can be determined by screening of combinatorial libraries and can be easily artificially synthesized. This is a huge advantage for most gastrointestinal cancers, which are difficult to treat due to their multidrug-resistance (*47*). Fortunately, several peptides have been found that have effective targeting ability, such as the arginine-glycine-aspartic acid (RGD) peptide (*77*), bombesin (BBN) (*78*) and gastrin-releasing peptide (GRP, a bombesin-like peptide) (*79*).

The RGD peptide has a binding high affinity to $\alpha_v\beta_3$ integrin receptors overexpressed on the surface of certain tumor cells (*80*) and of endothelial cells lining

the newly formed blood capillaries inside solid tumors (*81*). Different RGD peptides can be used as targeting delivery systems, such as c(RGDyK), c(RGDfK), [c(RGDyK)$_2$], RGD4C, and RGD10 (Figure 12) (*80*). Numerous studies used RGD modified PAMAM dendrimers to target tumor cells and tumor microvasculature (*82-84*). For instance, Shukla *et al. (82)* developed a G5 PAMAM dendrimer–RGD-4C peptide conjugate and studied its *in vitro* targeting efficacy to integrin receptor expressing cells. Similarly, Saijie *et al.* (*83*) covalently linked DOX to RGD-modified PAMAM dendrimer conjugates (an acid-sensitive cis -aconityl linkage was used to link DOX to the surface of the dendrimer). Their results demonstrated that RGD modified dendrimers significantly improved the therapeutic effect against murine B16 melanoma compared with the same dendrimer without RGD modification. Cyclic RGDs have also been attached to DOTA-conjugated mono, di-, and tetravalent dendrimeric alkynes for $\alpha_v\beta_3$ integrin targeting (*51*). The binding characteristics of these systems were evaluated *in vitro* and *in vivo* using human SK-RC-52 cells and the mice-bearing xenografted SK-RC-52 tumor model. It was shown through biodistribution studies that the tetrameric RGD-dendrimer showed the highest level of tumor targeting. These studies demonstrated that RGD-modified dendrimers could be used as a platform for therapy and imaging of tumor tissues overexpressing $\alpha_v\beta_3$ integrins.

There are obvious advantages of peptide targeting delivery systems. However, the inherent problem of these systems is that the stability of peptides in circulation is difficult to control. So it is important to make an appropriate design of these delivery systems to prevent or slow down the amide hydrolysis (*47*).

In general, the research involving dendrimers and targeted delivery has evolved well. However, more efforts are needed to develop a system that is effective and that is of low cost.

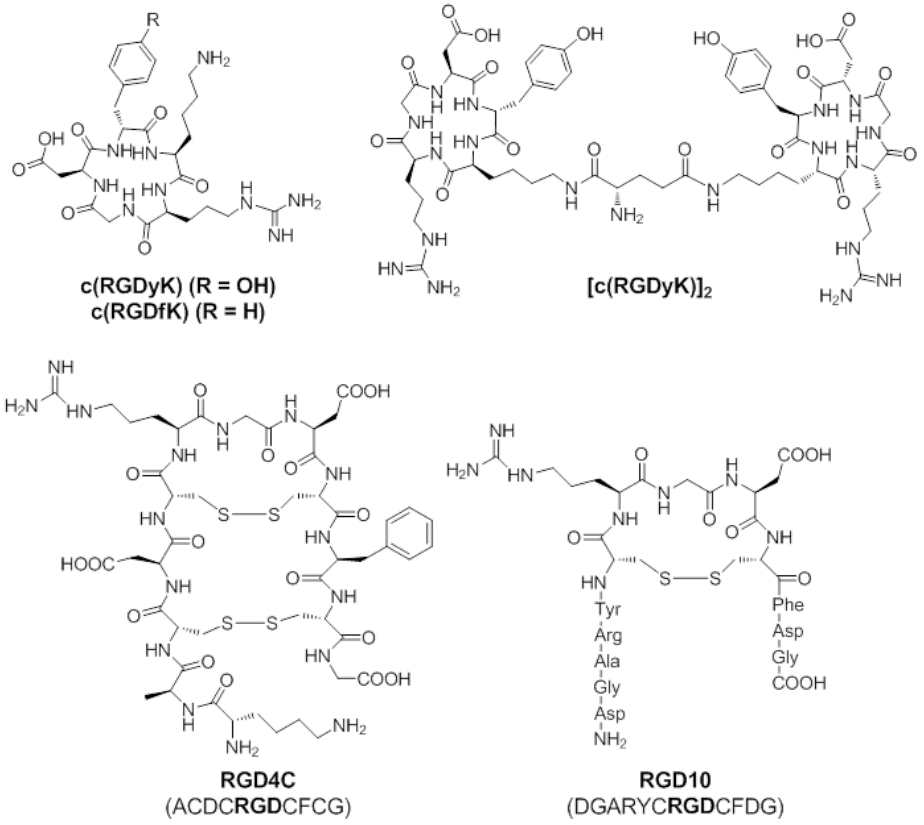

Figure 12 – Chemical structures of c(RGDyK), c(RGDfK), [c(RGDyK)$_2$], RGD4C, and RGD10. Adapted from ref. (*80*).

1.5 Host-Guest interactions

To better understand the influence of dendrimer terminal groups on the properties of dendrimer-based drug delivery systems, the interaction between drug molecules and dendrimers has been investigated via various techniques, such as Ultraviolet-visible (UV−vis) spectroscopy (*20*), high performance liquid chromatography (HPLC) (*16*) and NMR (*85*). Among all these methods, NMR techniques, including ^{1}H and ^{13}C NMR titrations, two-dimensional nuclear Overhauser enhancement spectroscopy (2D-NOESY), and diffusion-ordered spectroscopy (DOSY), have been demonstrated to be effective in studying the dendrimer host−drug guest interactions. Zhang *et al*. encapsulated DOX within G5.NHAc, G5.NGlyOH, and G5.SAH dendrimers (*86*). ^{1}H NMR, 2D-NOESY, and DOSY techniques were used to investigate the host-guest interactions of these

dendrimer/DOX complexes. The results showed that DOX was successfully incorporated into dendrimers although the exchange rate between free and coordinated DOX was high. Moreover, calculations based on DOSY experiments showed the diffusion coefficients of DOX, and proved that the interaction intensity between dendrimer and DOX follows the order of G5.NHAc/DOX > G5.NGlyOH/DOX > G5.SAH/DOX.

1.6 Objectives & General Strategy of the Thesis

The objective of the present study was to prepare RGD peptide-modified G5 PAMAM dendrimers for the encapsulation of the anticancer drug DOX for targeted delivery to cancer cells overexpressing the $\alpha_V\beta_3$ integrin. As shown in Figure 13, in the synthesis process, the thiolated RGD peptide was first linked to PEG (PEG in the form of NH_2-PEG-COOH) making use of MHS. The formed PEGylated RGD peptide with carboxyl end groups was covalently attached onto the G5 PAMAM dendrimers via 1-ethyl-3-(3-dimethylaminopropyl) carbodiimide hydrochloride (EDC) coupling chemistry. After linking FI and acetylation of the remaining dendrimer terminal amines, multifunctional FI- and RGD- modified G5 PAMAM dendrimers were formed. These multifunctional dendrimers were used to encapsulate DOX. The interactions between the drug molecules and the modified dendrimers were then investigated using NMR techniques, including ^{1}H NMR, 2D-NOESY, and DOSY. The release kinetics of DOX was also investigated. Finally, the targeting and therapeutic capabilities of these nanomaterials were investigated *in vitro* using U87-MG cells that overexpress the $\alpha_V\beta_3$ integrin.

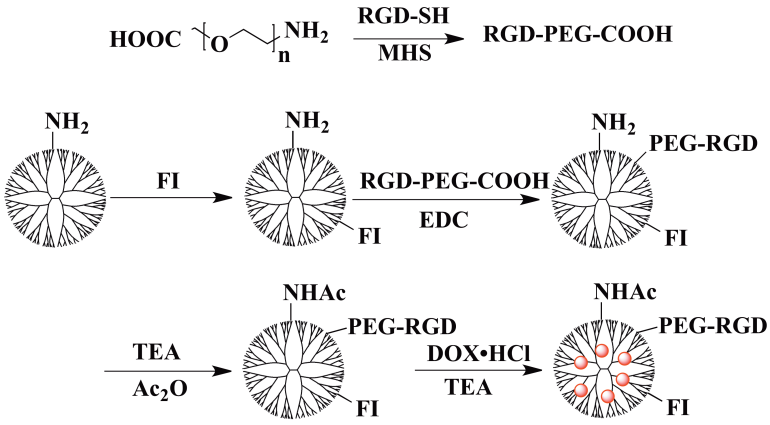

Figure 13 – Synthesis procedure of G5.NHAc-FI-PEG-RGD/DOX.

CHAPTER 2 – MATERIALS AND METHODS

CHAPTER 2 – MATERIALS AND METHODS

2.1 Materials and reagents

G5 PAMAM dendrimers possessing ethylenediamine cores and amine termini (PAMAM G5.NH_2) were purchased in methanol solution from Dendritech Inc.. Acetic anhydride (purity > 98%) was purchased from Panreac. Triethylamine (TEA) (purity > 99%) was purchased from MERCK. PEG having on one end an amine group and on the other end a carboxyl group (NH_2-PEG-COOH, M.W. = 2000 g/mol) was purchased from Yarebio (China). A cyclic RGD peptide with molecular weight of 706.8 g/mol was purchased from GenicBio (Shanghai, China). All other chemicals were obtained from SIGMA-ALDRICH unless otherwise stated and used as received. Cell culture dishes were from Nunc. The dialysis membranes were from Spectrum® labs and the filters used for solution sterilization were from VWR™ with a pore size of 0.22μm. U87-MG cells were from European Collection of Cell Cultures (ECACC) (Salisbury, UK).

2.2 Synthesis of G5.NHAc-FI-PEG-RGD dendrimers

HOOC-PEG-RGD was synthesized by the following method. NH_2-PEG-COOH (63 mg, 0.03 mmol) was dissolved in 3 mL dimethyl sulfoxide (DMSO), then MHS (9.25 mg, 0.03 mmol) in DMSO (3 mL) was added into the NH_2-PEG-COOH solution under vigorous magnetic stirring at room temperature for 8 h. Afterwards, RGD (21.2 mg, 0.03 mmol) in DMSO (4 mL) was added into the solution at room temperature for 24 h. The reaction mixture was dialyzed against distilled water (3 times, 3 L) through a 1,000 MWCO membrane for 24 h, followed by lyophilization.

To conjugate FI and PEG-RGD to G5 PAMAM dendrimer, PAMAM G5.NH_2 dendrimers (57.7 mg, 0.002 mmol) in methanol solution were dissolved in 5 mL of PBS 0.1 M (pH 7.4). FI (11.68 mg, 0.03 mmol) was dissolved in DMSO (5 mL) and

added dropwise into the dendrimer PBS buffer solution at room temperature and stirred vigorously for 12 hours. The reaction mixture was first dialyzed against PBS buffer and later against distilled water through a 12,000 MWCO membrane for 2 days to remove any excess of free FI. This was followed by lyophilization to get the G5.NH_2-FI dendrimers. The RGD-PEG-COOH (20 mg, 0.0087 mmol) was then reacted with 14-fold excess of EDC in DMSO for two hours to activate the –COOH functional groups. This solution was then added dropwise to the aqueous solution of the G5.NH_2-FI dendrimer (19.56 mg, 0.00058 mmol) and reacted for two days. The same dialysis and lyphophilization steps were done in order to achieve pure G5.NH-FI-PEG-RGD.

The final synthesis step of the multifunctional dendrimer was to neutralize the remaining amine groups of the G5.NH_2-FI-PEG-RGD dendrimers. First, the G5.NH_2-FI-PEG-RGD dendrimer (10 mg, 0.000144 mmol) was dissolved in 5 mL DMSO. Then, TEA (7.27 mg, 0.07 mmol) and acetic anhydride (5.87 mg, 0.06 mmol) in 5 mL DMSO were slowly added into the dendrimer solution. This reaction was stirred at room temperature for 24 h. Afterwards, dialysis and lyophilization were followed to get clean/pure G5.NHAc-FI-PEG-RGD.

2.3 Characterization of G5.NHAc-FI-PEG-RGD

^{1}H NMR spectra of the starting materials (NH_2-PEG-COOH, MHS, RGD and the G5 PAMAM dendrimer), all the intermediate products and the final G5.NHAc-FI-PEG-RGD product were recorded using a Bruker Avance II$^+$ 400MHz NMR spectrometer. Samples were dissolved in 500-600 µL D_2O before measurements. UV-Vis spectra were performed using a Lambda 2 UV/Vis spectrometer (Perkin-Elmer). Samples were dissolved in 1 mL distilled water before measurements. Zeta-potential measurements were performed to measure the potential of modified dendrimers at three pH values (5.0, 7.0, and 10.0) using a Zetasizer Nano ZS system (Malvern) with a 633nm incident laser beam and a detection angle of 17°. Zeta potentials were calculated using the Smoluchowsky model for aqueous

suspensions.

2.4 Encapsulation of DOX within G5.NHAc-FI-PEG-RGD dendrimers

G5.NHAc-FI-PEG-RGD dendrimers (10 mg) were dissolved in 1.5 mL water. DOX hydrochloride (DOX·HCl) with 10 molar equivalents of dendrimers was dissolved in 300 μL methanol followed by adding 5 μL TEA to generate non-protonated DOX. Then the dendrimer aqueous solution was mixed with the non-protonated DOX solution for 12 hours, allowing the evaporation of the methanol solvent. After that, the mixture solution was centrifuged (5423 g for 10 min) in order to remove the precipitates, which were due to non-complexed free DOX. The supernatant was lyophilized to obtain the G5.NHAc-FI-PEG-RGD/DOX complex. The precipitate was saved and re-dissolved into 10 mL methanol for indirect determination of the encapsulated amount of DOX by UV-Vis analysis (Lambda 2 UV/Vis spectrometer, Perkin-Elmer).

2.5 In vitro drug release kinetic studies

A volume of either 2 mL pH = 7.4 PBS buffer or pH = 5 acetate buffer was used to dissolve the G5.NHAc-FI-PEG-RGD/DOX complex. 2 ml ethanol was used to dissolve free non-protonated DOX. Then, these three solutions were placed in dialysis bags with a MWCO of 12,000, and after well-sealed, the bags were immersed in 6 mL of pH = 7.4 PBS buffer, pH = 5 acetate buffer, and pH = 7.4 PBS buffer respectively. All the systems were kept at 37 °C. At specific time points, 1 mL of the buffer medium was taken out for analysis and the volume replenished with the corresponding buffer solution. UV-Vis spectroscopy was used to determine the DOX content in the removed aliquots.

2.6 Host-guest interactions of the dendrimer/DOX complex studies

One- and two-dimensional (NOESY, DOSY) NMR experiments were carried out using a Bruker DRX Avance I 400 MHz NMR spectrometer at the University of Debrecen (Hungary). In the case of the G5.NHAc-FI-PEG-RGD/DOX complex at pH = 5, 4 mg of G5.NHAc-FI-PEG-RGD dendrimer and 2.5 mg of DOX·HCl were co-dissolved within 500 μL of D_2O, then 2 μL TEA and 200 μL DCl were used to adjust pH ≈ 5.0. In the case of the G5.NHAc-FI-PEG-RGD/DOX complex at pH = 7.0, 4 mg of dendrimer, 2.5 mg of DOX·HCl and 0.1 μL of TEA were dissolved in D_2O. 2D-NOESY experiments were obtained with a mixing time of 200 ms and a relaxation delay of 1.7 s. Data were processed with cos2 window function in both f1 and f2 dimensions according to the Bruker protocols. Each of the NOESY spectral data was processed with Mestre Nova software. DOSY experiments were performed with the following parameters: diffusion time (Δ) = 50 ms, gradient pulse (δ) = 3 ms, and relaxation delay = 5 s. DOSY spectral data were processed in 1D and 2D modes with Mestre Nova software.

2.7 Cell biological evaluation

U87-MG cells (a human primary glioblastoma cell line in which the $\alpha_v\beta_3$ integrin receptors are overexpressed) were continuously grown in the cell culture dishes with Eagle's Minimum Essential Medium (EMEM) supplemented with 10% fetal bovine serum (FBS), 1% (v/v) of antibiotic and antimycotic 100x solution (AA), 1% (v/v) of Non essential amino acids 100x (NEAA), 1% (v/v) of Sodium pyruvate 100x (SP) and 1% (v/v) of L-Glutamine (Glut) 100x. All the reagents mentioned here were purchased from Gibco. The culture was maintained at 37 °C in a wet incubator with 5 % CO_2, and the medium was replaced every 3 days.

To check if the G5.NHAc-FI-PEG-RGD/DOX complex was therapeutically active, one day before experiments, cells were plated into 96-well plates at a density of 1×10^4 cells per well in the EMEM complete medium. The next day, the medium

was replaced with fresh EMEM complete medium containing free DOX·HCl (5 μM) or G5.NHAc-FI-PEG-RGD/DOX complex at the same DOX concentration in PBS buffer (10 μL) and then the cells were incubated for 48 h at 37 °C. After treatment with DOX or dendrimer/DOX complexes, cell morphology was observed by optical microscopy (Nikon Eclipse TE 2000E inverted microscope). The magnification was set at 100× for all samples. After morphology observations, 3-(4,5-dimethylthiazol-2-yl)-2,5-diphenyltetrazolium bromide (MTT) assay was performed to quantify the viability of the cells. Note that for the DOX encapsulation and release studies, water-insoluble DOX was used, while for cell biological evaluation, water-soluble DOX·HCl was used as a control to check the therapeutic activity of the free drug.

To investigate if the uptake of G5.NHAc-FI-PEG-RGD/DOX was receptor-mediated, one group of the U87-MG cells was pre-treated with 100 μL of RGD solution (2 μM in serum free medium) to block the $\alpha_v\beta_3$ integrins. Meanwhile, the other groups were treated with serum free medium. After 1 h, all the media was replaced with fresh complete medium (90 μL), and the G5.NHAc-FI-PEG-RGD/DOX complex with DOX concentration of 5 μM in PBS buffer (10 μL) was added to the cells and incubated for 4 h. Afterwards, all the media in the wells containing dendrimer/DOX complexes were totally taken out and replenished with the same volume of fresh complete medium. The cells were then incubated for 48 h at 37°C before performing the MTT assay. In parallel cell samples, after 4 h incubation with the G5.NHAc-FI-PEG-RGD /DOX complex, the culture medium was removed, and the cell nuclei were stained with 2.5 mg/mL 4’,6-diamidino-2-phenylindole (DAPI) at room temperature for 35 min and fixed with 3.7 % formaldehyde for 20 min. After, the cells were rinsed three times with PBS and three times with ultrapure water. The intracellular uptake of free DOX·HCl or G5.NHAc-FI-PEG-RGD/DOX complexes was observed by fluorescence microscopy (Nikon Eclipse TE 2000E inverted microscope).

The MTT assay was used to quantify cell viability. The metabolically active cells were detected by adding a 200 μL volume of MTT (5 mg/mL in EMEM medium) to each well. After 3 h incubation, the MTT solution in each well was replaced with 200 μL of DMSO to dissolve the formazan crystals. Then, the plates were read at 550 nm using a microplate reader (model Victor3TM 1420, PerkinElmer). The mean and the standard deviation were reported (4 replicas were done).

2.8 Statistical analysis

One way ANOVA statistical analysis was performed to evaluate the significance of the experimental data. 0.05 was selected as the significance level, and the data was indicated with (*) for $p < 0.05$, (**) for $p < 0.01$, and (***) for $p < 0.001$, respectively.

CHAPTER 3 – RESULTS AND DISCUSSION

CHAPTER 3 – RESULTS AND DISCUSSION

3.1 Synthesis and characterization of G5.NHAc-FI-PEG-RGD

G5 PAMAM dendrimers were selected for the synthesis of multifunctional drug carriers due to their relative small size, comparable to hemoglobin (5.4 nm), and numerous terminal amine groups for multiple conjugation reactions (*87, 88*). The FI moieties covalently attached to the dendrimer surface were used to detect by fluorescence the intracellular uptake of the dendrimer carriers. The RGD peptide was attached onto the dendrimer surfaces so as to target for the cancer cells that overexpress integrin $\alpha_v\beta_3$ (*89*). The final acetylation is a key step to improve the biocompatibility of the dendrimers and to minimize their non-specific binding to cell membranes.

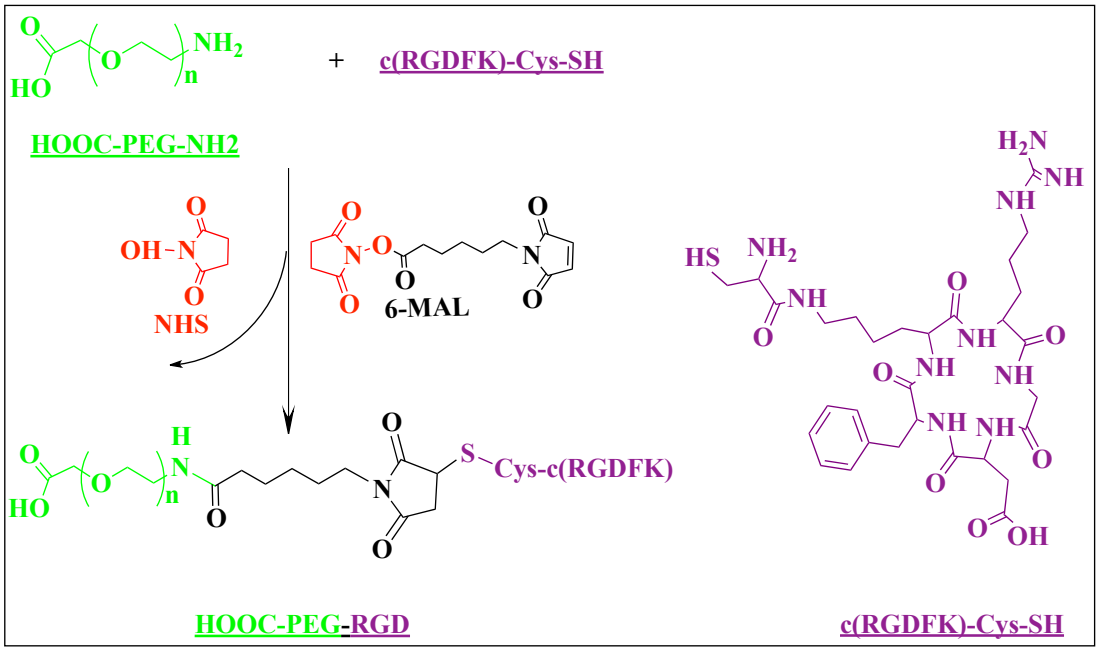

Figure. 14 – Synthesis of HOOC-PEG-RGD.

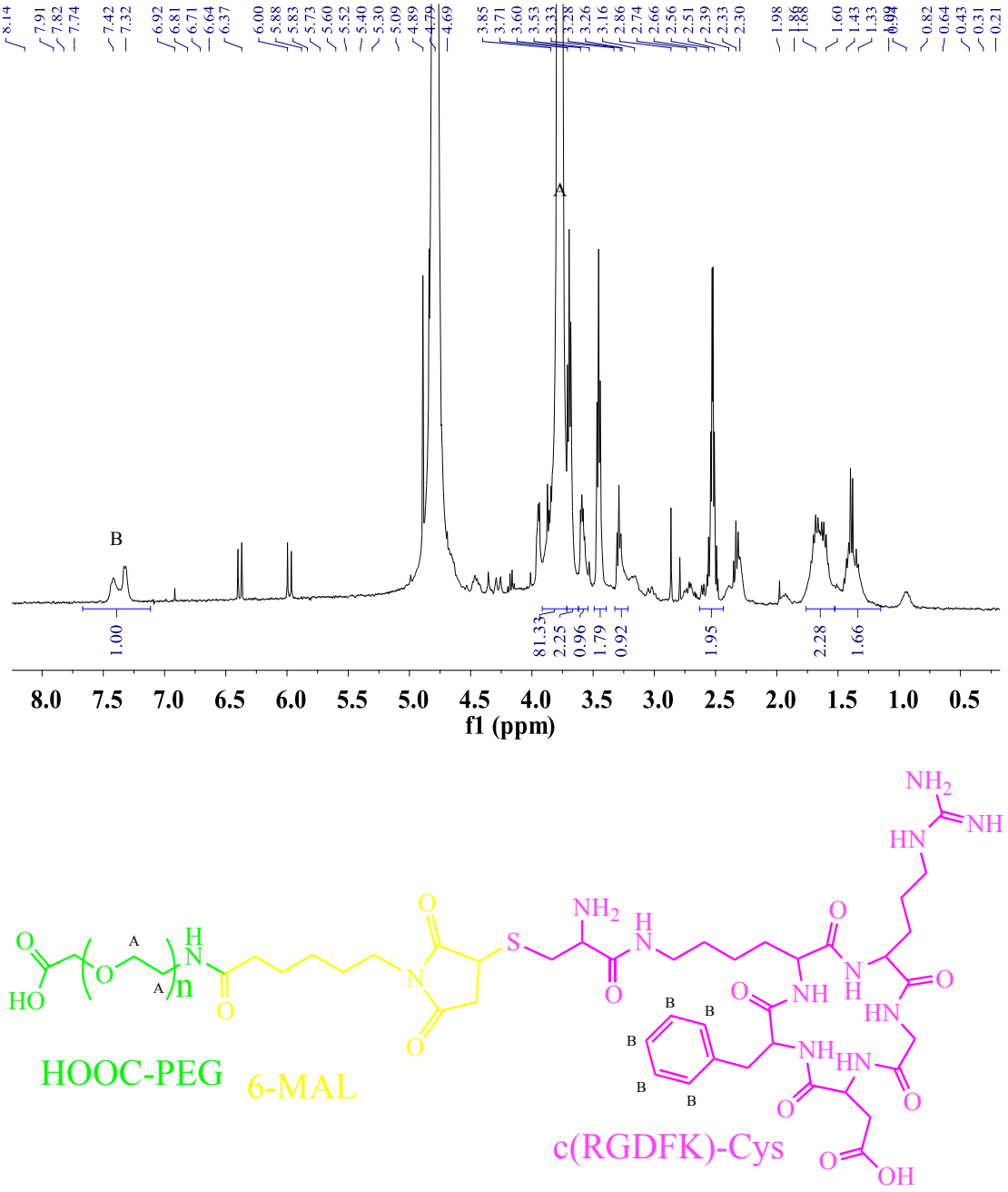

Figure 15 – ^{1}H NMR spectrum of HOOC-PEG-RGD in D_2O (with integration and identifications of peaks).

The overall synthesis process is depicted in Figure 13. So, the first step was to synthesize HOOC-PEG-RGD from HOOC-PEG-NH_2 and a cyclic RGD peptide (Figure 14). The ^{1}H NMR spectra of HOOC-PEG-NH_2, MHS and RGD are presented in ANNEX I (Figure 40, 41 and 42, respectively). In the ^{1}H NMR spectrum of

HOOC-PEG-RGD in D_2O (see Figure 15), we can see the characteristic peak of the PEG methylene protons (-OCH_2CH_2, δ=3.7 ppm) and the characteristic peaks of RGD around 7.3-7.4 ppm. Since during dialysis, free RGD was cleared out from the reaction mixture, we suppose that the RGD peaks in the ^{1}H NMR spectrum of HOOC-PEG-RGD represent only the RGD molecules that were linked to the PEG molecules. However, the PEG peaks presented in the spectrum correspond to both free and linked PEG. Thus, based on the integration of the relevant peaks, we calculated that 0.3 RGD moieties were linked to each PEG.

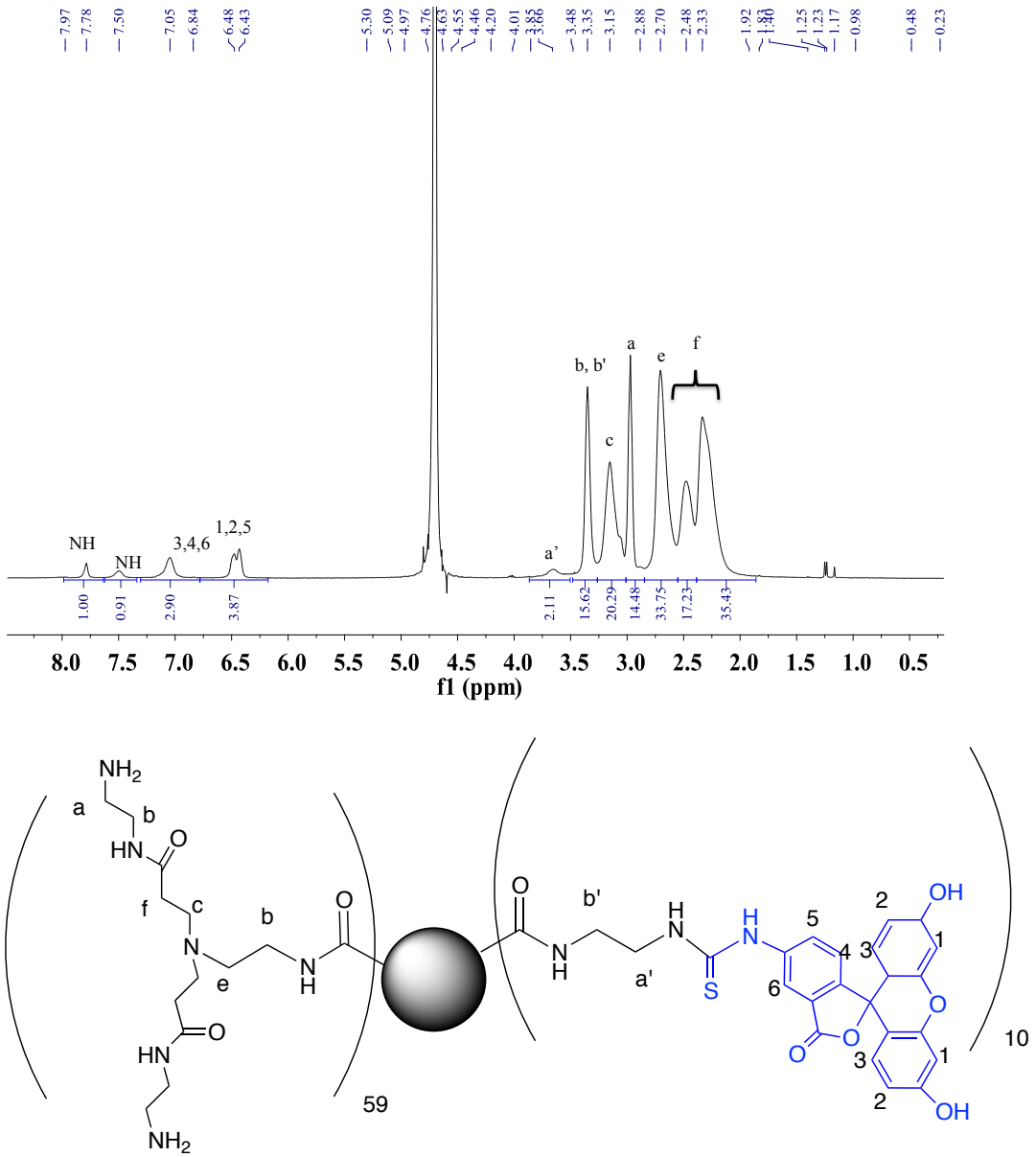

Figure 16 – ^{1}H NMR spectrum of PAMAM G5.NH_2-FI dendrimer in D_2O.

In a second step, the PAMAM G5.NH_2-FI dendrimer was synthesized and characterized. The ^{1}H NMR spectrum of the G5 PAMAM dendrimer is presented in ANNEX I (Figure 43). The characteristic peak at 3.75 ppm (Ha') in the ^{1}H NMR spectrum, corresponding to the aliphatic protons of $CH_2NHC{=}S$, confirmed the formation of a thiourea linkage between the G5 PAMAM dendrimer and the FI moeity (see Figure 16). The comparison between aromatic proton peaks at 6.5 ppm (1,2,5) and at 7.1 ppm (3,4,6) of FI and the methylene groups of the G5 PAMAM dendrimer (Ha) suggest that 10 FI moieties were conjugated to each dendrimer.

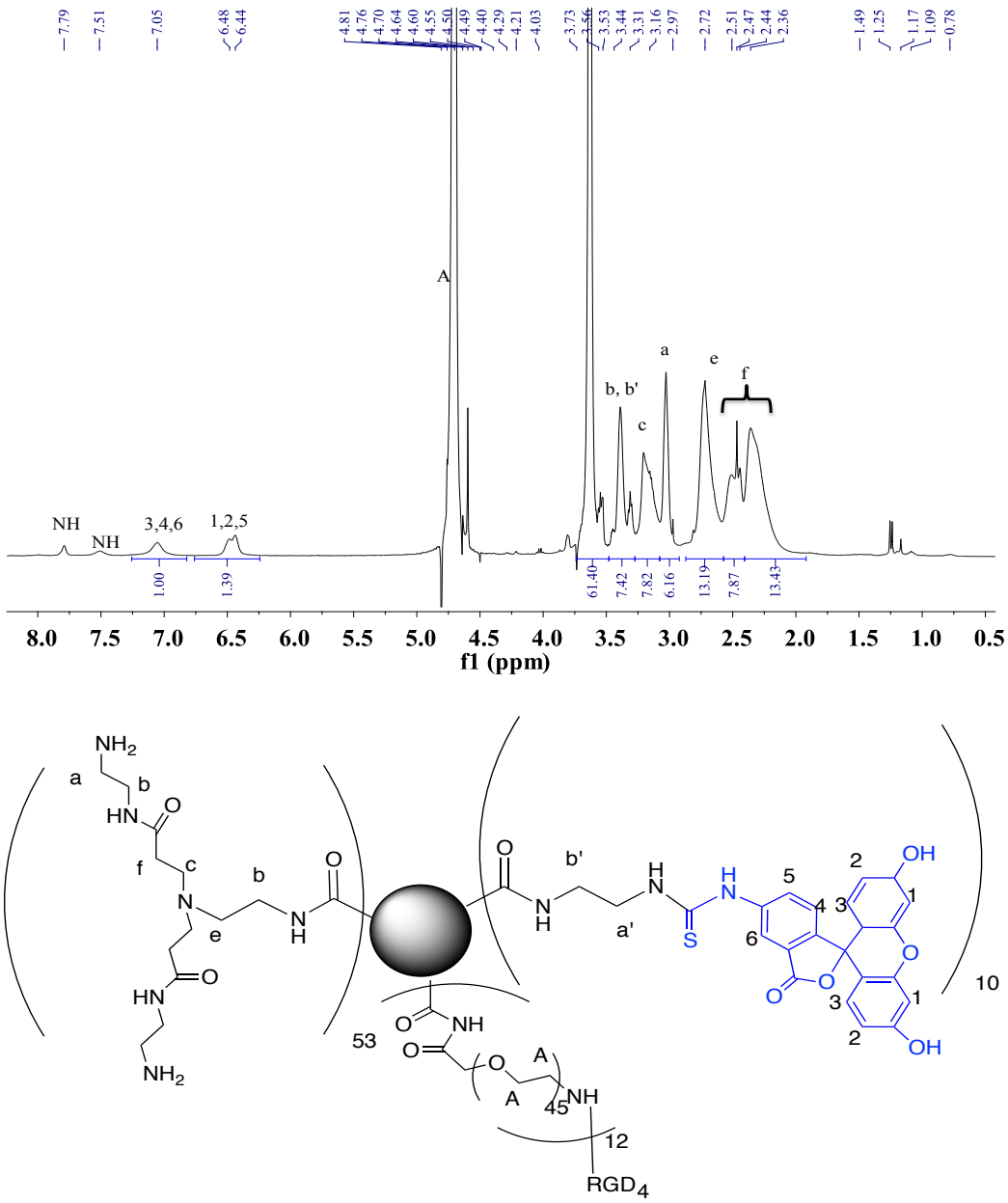

Figure 17 – ^{1}H NMR spectrum of G5.NH_2-FI-PEG-RGD in D_2O.

Finally, HOOC-PEG-RGD was reacted with PAMAM G5.NH_2-FI to give the G5.NH_2-FI-PEG-RGD product. Following the identification of the characteristic peaks of PEG, the G5 PAMAM dendrimer and FI, and after integration, it was found that 12 PEG and 4 RGD moieties were attached to each dendrimer molecule. According to the literature, 2-3 RGD peptides per dendrimer are sufficient for effective targeting (*82*).

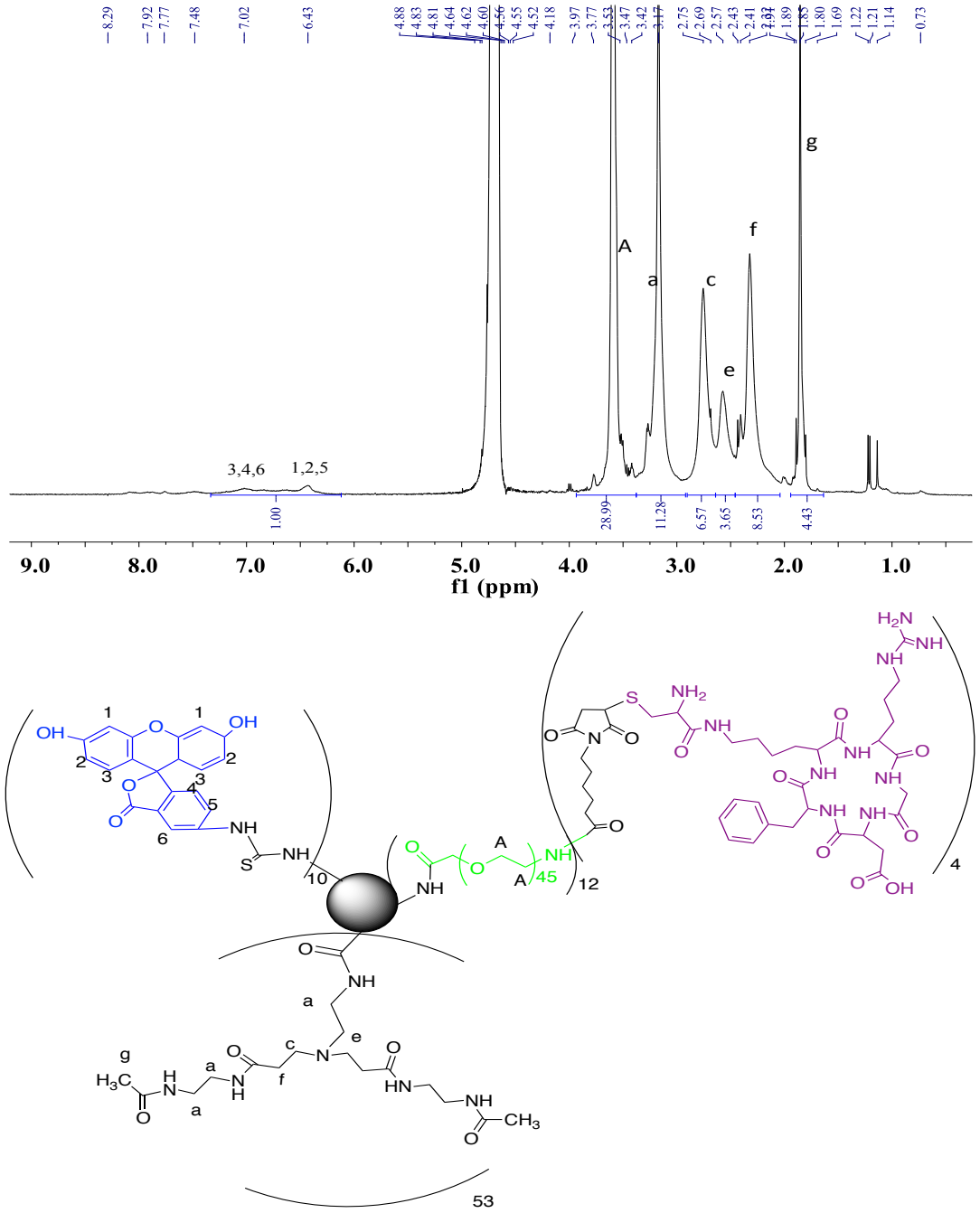

Figure 18 – ^{1}H NMR spectrum of G5.NHAc-FI-PEG-RGD in D_2O.

Figure 18 shows the ^{1}H NMR spectrum and peak assignment of the final G5.NHAc-FI-PEG-RGD conjugate obtained after acetylation of the previous compound. The characteristic proton peaks at 3.6 ppm that correspond to PEG can be clearly seen. Furthermore, there are overlapping signals in the aromatic region from both the FI and the phenyl ring of the peptide apart from the overlapping expected from the aliphatic signals of the dendrimer and some aliphatic signals from the peptide. After the final acetylation step, the appearance of a new peak at 1.87 ppm was detected which was assigned to the $-CH_3$ protons of the acetyl group, indicating the complete conversion of the remaining terminal amines to acetamides, in agreement with previous literature (*1*).

UV-Vis spectroscopy was further used to characterize the synthesized G5NHAc-FI-PEG-RGD dendrimer conjugates (Figure 19). For comparison, UV-Vis spectra of HOOC-PEG-RGD, G5.NH_2-FI, and G5.NH_2-FI-PEG-RGD were also included. HOOC-PEG-RGD shows a characteristic peak for the conjugated peptide at λ_{max} = 275 nm, which is in accordance with the data from the literature (*82*). G5.NH_2-FI displays a characteristic peak at 500 nm due to the conjugated FI moieties. The G5.NH_2-FI-PEG-RGD and the G5.NHAc-FI-PEG-RGD conjugates both exhibited the featured absorption of FI (500 nm), indicating the success of FI conjugation.

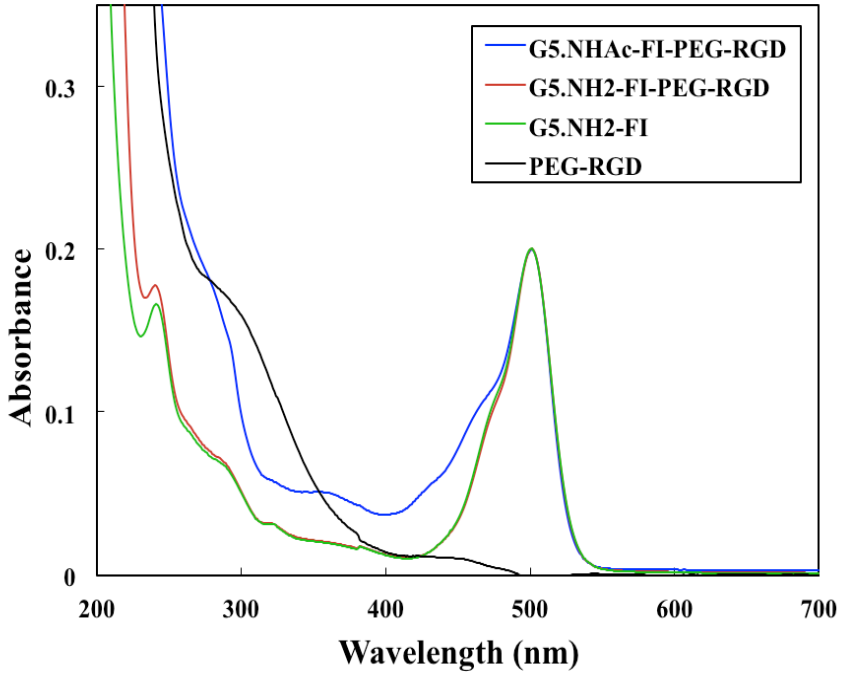

Figure 19 – UV-Vis spectra of HOOC-PEG-RGD, G5.NH_2-FI, G5.NH_2-FI-PEG-RGD and G5.NHAc-FI-PEG-RGD.

3.2 Encapsulation of DOX within the G5.NHAc-FI-PEG-RGD dendrimers

The neutralization of DOX·HCl to form DOX enables efficient encapsulation of the drug within the relatively hydrophobic interior of the dendrimers. Since free DOX has low solubility, the formed dendrimer/DOX complexes are expected to have improved water-solubility and thus enhanced bioavailability. The formed G5.NHAc-FI-PEG-RGD/DOX complexes were characterized by UV-Vis spectroscopy (Figure 20). The UV-Vis spectra of DOX dissolved in ethanol and G5.NHAc-FI-PEG-RGD dendrimers without DOX were also recorded for comparison. It is clear that DOX shows a strong absorption peak at 481 nm. After DOX encapsulation, the G5.NHAc-FI-PEG-RGD/DOX complexes have an absorption enhancement at 481 nm when compared with the G5.NHAc-FI-PEG-RGD dendrimers without DOX under a similar dendrimer concentration. This indicates that

DOX has been successfully encapsulated within the G5.NHAc-FI-PEG-RGD dendrimers.

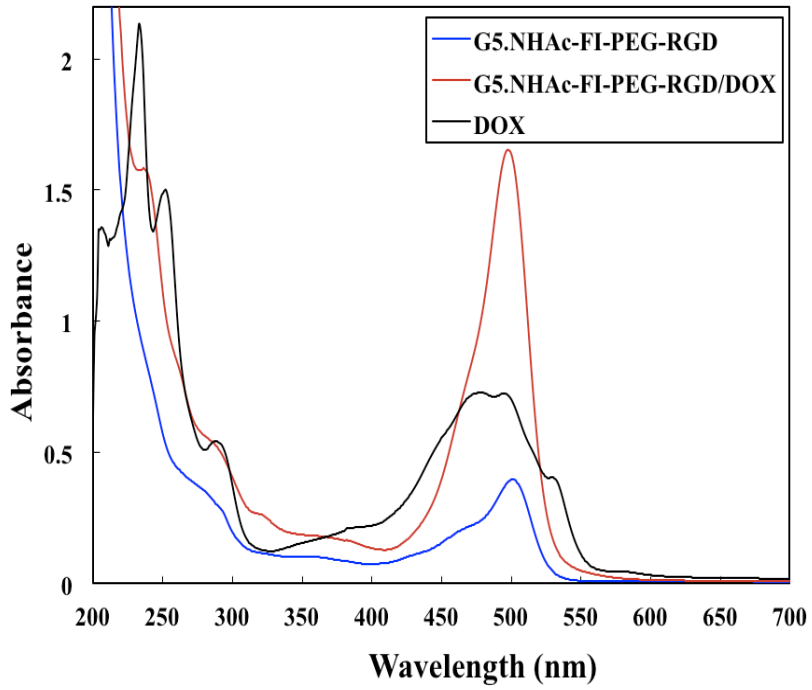

Figure 20 – UV-Vis spectra of free DOX dissolved in ethanol, G5.NHAc-FI-PEG-RGD dendrimers dissolved in water, and G5.NHAc-FI-PEG-RGD/DOX complexes dissolved in water.

3.2.1 STUDY OF THE PAYLOAD OF DOX PER DENDRIMER

The payload of DOX encapsulated within the G5.NHAc-FI-PEG-RGD dendrimers was obtained by measurement of the non complexed free DOX in solution that was recovered by centrifugation, redissolved and analyzed by UV-Vis spectroscopy.

3.2.1.1. Standard curve of DOX in pH = 7.4 PBS buffer.

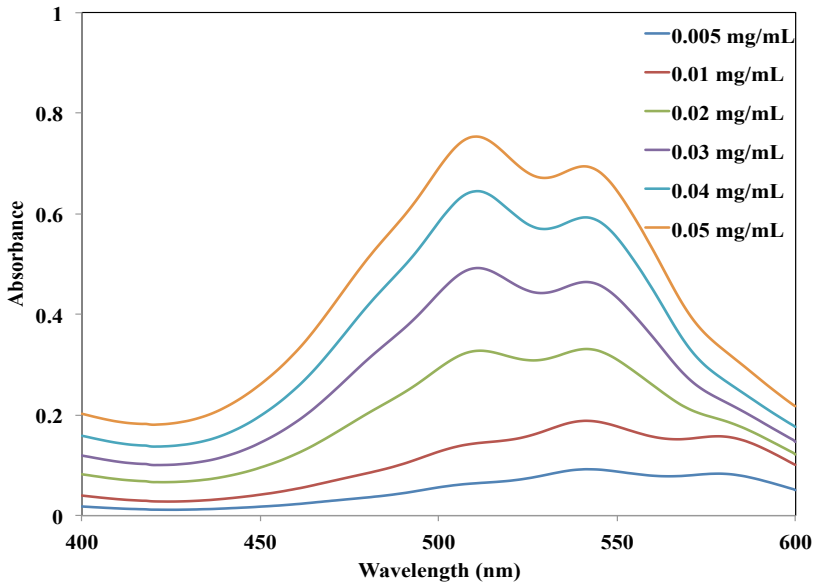

Figure 21 – UV-Vis spectra of DOX in pH = 7.4 PBS buffer.

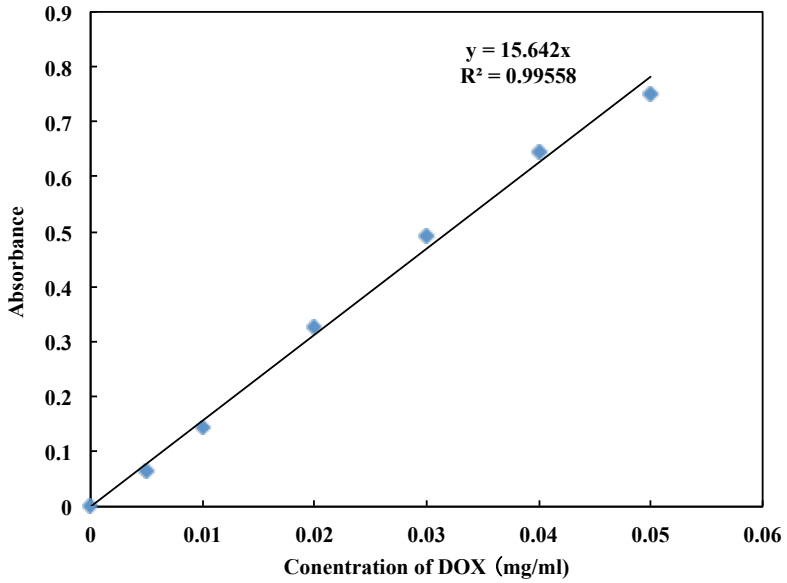

Figure 22 – Standard curve of DOX in pH = 7.4 PBS buffer.

A 5 µL volume of TEA was mixed with pH = 7.4 PBS buffer. DOX·HCl was then dissolved in this buffer in order to get 0.005, 0.01, 0.02, 0.03, 0.04 and 0.05 mg/mL DOX solutions. Using UV-Vis absorbance, λmax = 510 nm was recorded for DOX in PBS at pH = 7.4 (see Figure 21). The standard curve of DOX in PBS at pH = 7.4 was then constructed (see Figure 22; y = 15.642x and R^2 = 0.99558).

3.2.1.2. Standard curve of DOX in pH = 5 acetate buffer.

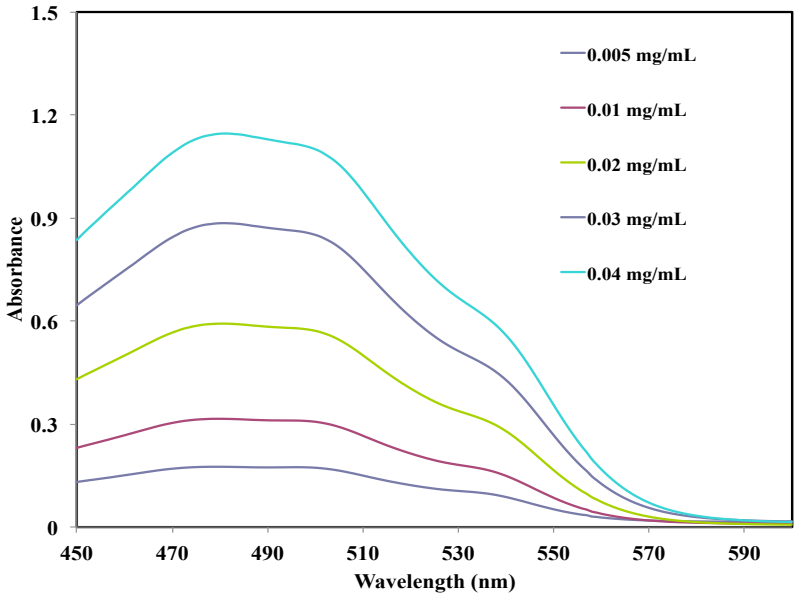

Figure 23 – UV-Vis spectra of DOX in pH = 5 acetate buffer.

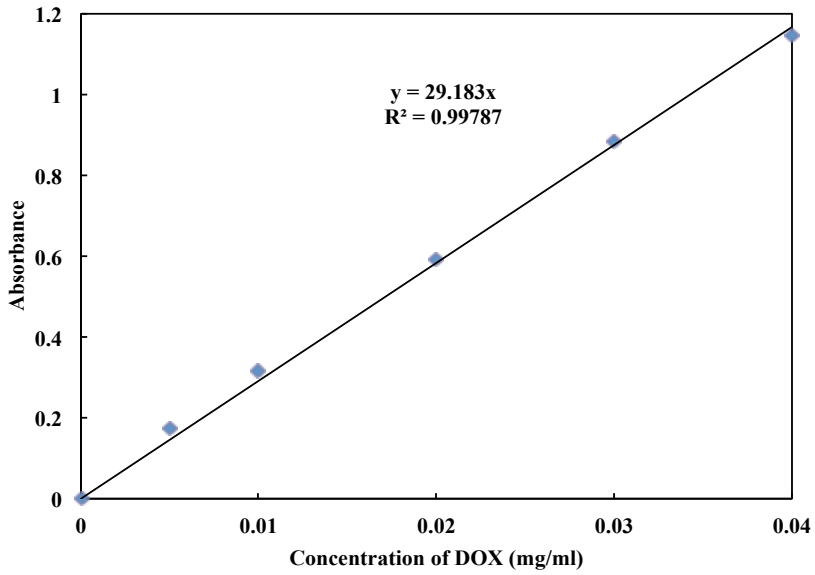

Figure 24 – Standard curve of DOX in pH = 5 acetate buffer.

The method described in Section 3.2.1.1 was used to make the standard curve of DOX in acetate buffer at pH = 5. From Figure 23 it is clear that λmax = 481 nm for DOX in acetate buffer at pH = 5. From the standard curve of DOX in acetate buffer at pH = 5 illustrated in Figure 24, y = 29.183x and $R^2 = 0.99787$.

3.2.1.3. Standard curve of DOX in methanol.

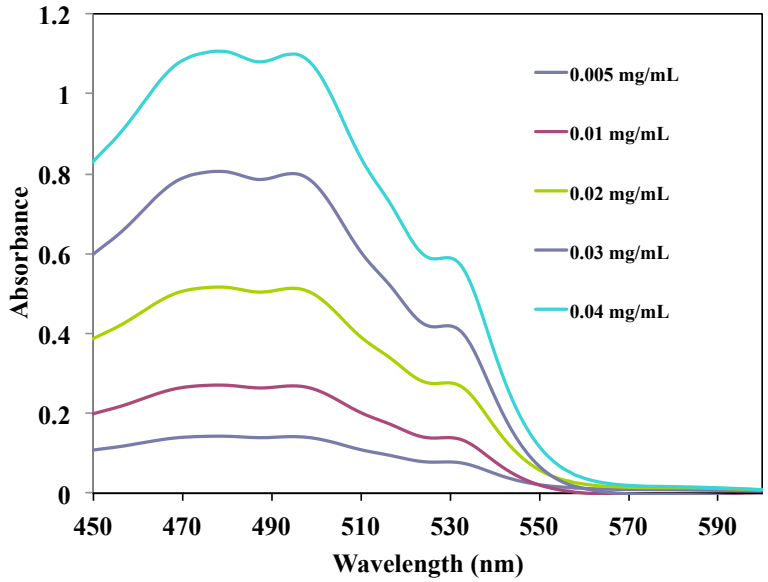

Figure 25 – UV-Vis spectra of DOX in methanol.

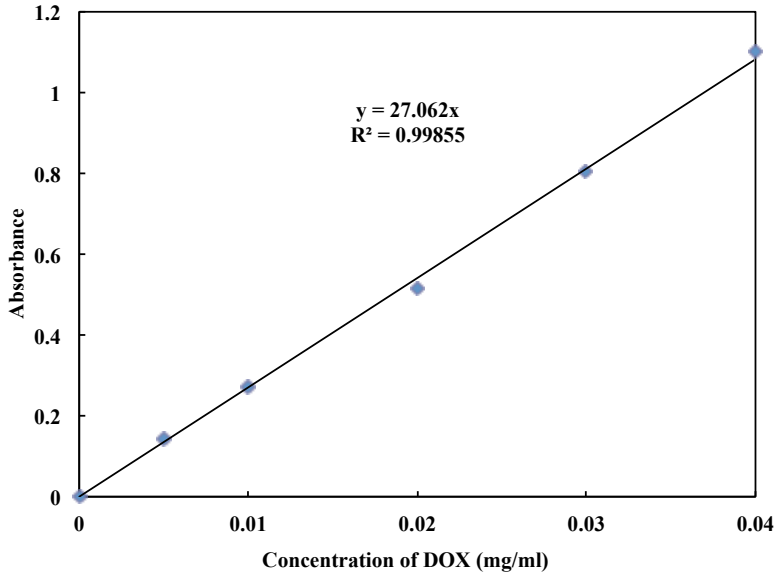

Figure 26 – Standard curve of DOX in methanol.

Again, the same method as that described in Section 3.2.1.1 was used to construct the standard curve of DOX in methanol. From the UV-Vis spectra shown in Figure 25, λmax = 479 nm for DOX in methanol. From the standard curve of DOX in methanol shown in Figure 26, y = 27.062x and $R^2 = 0.99855$.

3.2.1.4. Indirect calculations of the payload of DOX into the dendrimers.

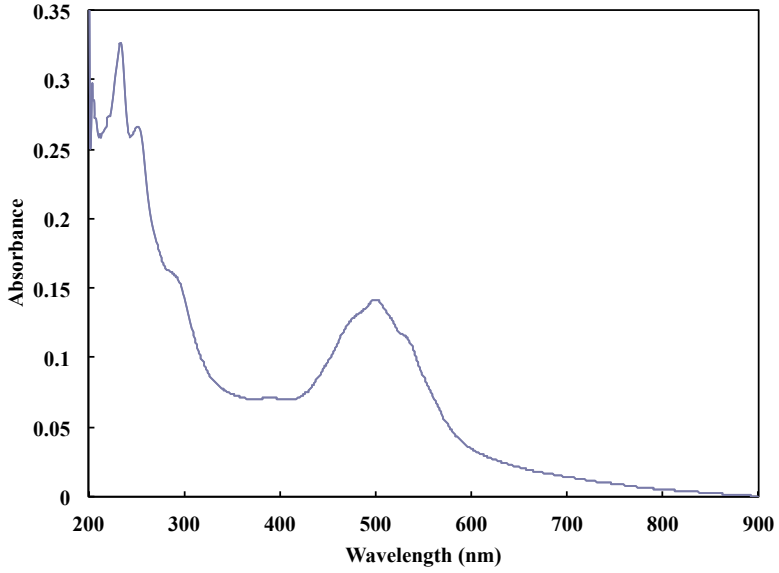

Figure 27 – UV-Vis spectrum of free DOX in the precipitate.

Note that the experiment investigating the encapsulation of DOX into the dendrimers was repeated 3 times. While we only show the results for one experiment here, the calculations for determining (i) the number of DOX molecules inside the dendrimer, (ii) the encapsulation efficiency, and (iii) the drug loading efficiency were based on the results of the three experiments.

In the synthesis procedure, G5.NHAc-FI-PEG-RGD dendrimers (11.65 mg) and DOX·HCl (0.838 mg) were used. After centrifugation (5423 g for 10 min), the precipitate (free DOX) was collected and dissolved into 10 mL methanol for UV-Vis analysis. Since the concentration of DOX was still too high to be analyzed by UV-Vis, 0.2 mL of the DOX solution was mixed with 0.8 mL methanol. The absorbance of DOX was then measured to be 0.14187 (see Figure 27). According to the standard curve of DOX in methanol, the mass of DOX precipitated was 0.263 mg. Therefore, the loaded DOX was 0.585 mg. Based on equations (1) and (2) presented below, the encapsulation efficiency (%) and drug loading efficiency (%) results were determined (see Table 1).

Encapsulation efficiency (%) = 100 x $m_{\text{drug in nanoparticles}} / m_{\text{total drug}}$ (1)

Drug loading efficiency (%) = 100 x $m_{\text{drug in nanoparticles}} / m_{\text{nanoparticles}}$ (2)

Table 1 – Payload of DOX per G5.NHAc-FI-PEG-RGD denrimer.

Material	Number of DOX inside one dendrimer	Encapsulation efficiency (%)	Drug loading efficiency (%)
G5.NHAc-FI-PEG-RGD	6	69±4	5±3

Approximately six DOX molecules were found to be complexed with each G5.NHAc-FI-PEG-RGD dendrimer, a larger number than that reported for acetylated G5 dendrimers modified with FA and FI in a previous work (*1*). According to the explanation in the literature (*90*), this may be because the hydrophilic PEG chains induce less steric hindrance than that induced by the relatively hydrophobic moieties of either FI or FA attached onto the dendrimer surface. The encapsulation efficiency was 69±4% and the drug loading efficiency was 5±3%.

3.2.2 STUDY OF THE STABILITY AND ZETA POTENTIAL OF THE DENDRIMER/DOX COMPLEX

The stability of the G5.NHAc-FI-PEG-RGD/DOX complexes is very important for their biological applications. As can be seen in Figure 28, the lyophilized powders of the G5.NHAc-FI-PEG-RGD dendrimers without DOX and the G5.NHAc-FI-PEG-RGD/DOX complexes could be dissolved in aqueous solution. As expected, the G5.NHAc-FI-PEG-RGD dendrimer solutions present different colors relative to the corresponding G5.NHAc-FI-PEG-RGD/DOX complexes. This difference in color is due to the presence of DOX in the G5.NHAc-FI-PEG-RGD/DOX complexes. This phenomenon suggests that the G5.NHAc-FI-PEG-RGD/DOX complexes have similar colloidal stability to that of the G5.NHAc-FI-PEG-RGD dendrimers without the drug under the selected pH conditions. In addition, their aqueous solutions showed no precipitate for at least two months at room temperature under the different pH conditions (pH = 5.0, 7.0, and 10.0).

The zeta potentials of the G5.NHAc-FI-PEG-RGD dendrimers and the

G5.NHAc-FI-PEG-RGD/DOX complexes at the different pH conditions are listed in Table 2. This information is important to understand the cellular interactions of the complexes. The smaller values at pH = 7.0 for both dendrimers and complexes compared to those at pH = 5.0 indicates that a portion of the dendrimer tertiary amines were protonated at pH = 5.0 (*91*). The change of the surface potential of both the dendrimers and complexes with pH followed the same trend as that of G5.NHAc-PEG-RGD dendrimers described in a previous work (*20*).

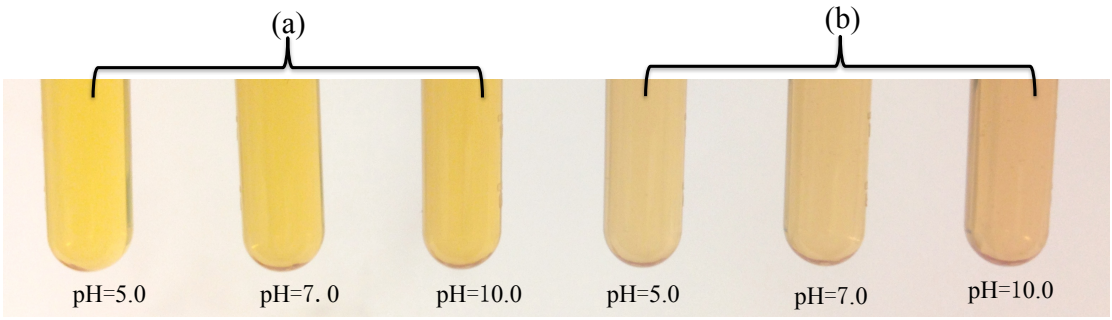

Figure 28 – Photographs of the aqueous solutions of G5.NHAc-FI-PEG-RGD dendrimers (a) and G5.NHAc-FI-PEG-RGD/DOX complexes (b) under different pH conditions.

Table 2 – Zeta potential values of G5.NHAc-FI-PEG-RGD dendrimers and G5.NHAc-FI-PEG-RGD/DOX complexes under different pH conditions.

Materials	Surface potential		
	pH = 5.0	pH = 7.0	pH = 10.0
G5.NHAc-FI-PEG-RGD Dendrimers	24.6 ± 1.7	1.7 ± 0.2	−33.2 ± 0.7
G5.NHAc-FI-PEG-RGD/DOX complex	20.4 ± 0.6	0 ± 0.1	−26.8 ± 1.0

3.3 In vitro release kinetic studies

The *in vitro* release study of DOX from the G5.NHAc-FI-PEG-RGD/DOX complexes was performed in either PBS buffer (pH = 7.4) or acetate buffer (pH = 5.0) media at 37 °C. In each case, the cumulative release of DOX from the complexes

showed that the drug was released in a sustained manner. Moreover, the release of DOX from the G5.NHAc-FI-PEG-RGD/DOX complexes followed a biphasic pattern that was characterized by an initial fast release followed by a sustained release profile (Figure 29). In contrast, the free DOX dissolved in ethanol was quickly released from the dialysis bag into the outer PBS buffer phase. In fact, about 80 % free DOX was released within just 2 h. In the case of G5.NHAc-FI-PEG-RGD/DOX in acetate buffer (pH = 5), about 10 % of the drug was released from the complex within 1 h, and about 21 % of the DOX was released within 24 h. In comparison, the drug release rate was observed to increase for the G5.NHAc-FI-PEG-RGD/DOX complex in PBS buffer pH 7.4), with about 35 % of the DOX being released within 1 h and approximately 57 % of the drug being released within 24 h. The prolonged release profile of DOX from the complexes under the two different buffer conditions implies that the dendrimer molecules are extremely useful for effective encapsulation and retention of the DOX drug. The release rate of DOX from the complexes at pH = 7.4 was higher than that at pH = 5.0. This could be due to the fact that under acidic pH conditions, the protonated DOX molecules are unlikely able to form strong hydrogen bonding with the dendrimer terminal functional groups (nonprotonated amines and terminal polar C-O-C bonds of the PEG moieties), leading to a slower release of DOX. In contrast, under slightly basic conditions at pH 7.4, the DOX molecules are able to form strong hydrogen bonding with the dendrimer terminal functional groups, resulting in a faster release rate of the drug from the dendrimer interior.

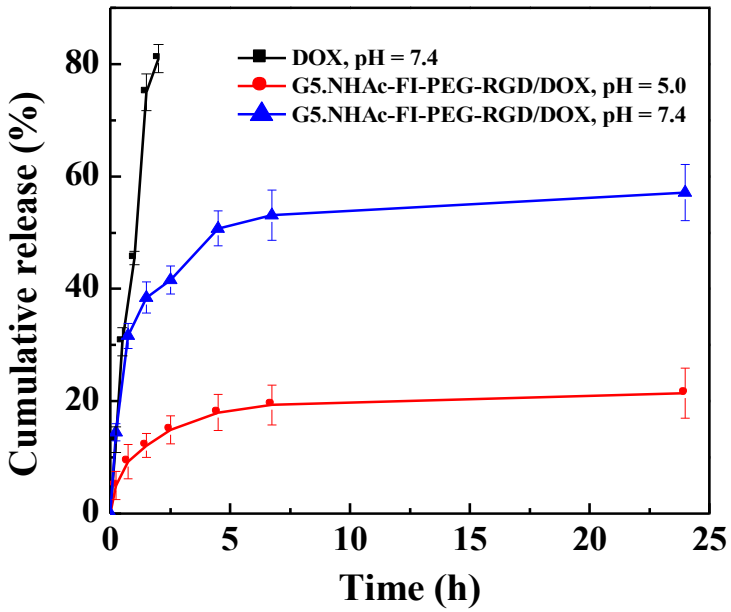

Figure 29 – Cumulative release of DOX from G5.NHAc-FI-PEG-RGD/DOX complexes in PBS buffer (pH = 7.4) and acetate buffer (pH = 5.0) at 37 °C. The free DOX was dissolved in ethanol against PBS buffer (pH = 7.4) as a control. The data is expressed as mean = S.D. (n = 3).

3.4 Host-guest interactions in the G5.NHAc-FI-PEG-RGD/DOX complex

3.4.1 ^{1}H NMR SPECTROSCOPY OF THE G5.NHAc-FI-PEG-RGD/DOX COMPLEX

To better understand the *in vitro* drug release results, and the influence of dendrimer terminal groups on the properties of dendrimer-based drug delivery systems, NMR techniques have been used to investigate the interaction between drug molecules and dendrimers (*85*).

^{1}H NMR experiments were performed to evaluate the influence of the pH on the interaction between the G5.NHAc-FI-PEG-RGD dendrimer and DOX·HCl in D_2O (Figure 30). Compared with the ^{1}H NMR of G5.NHAc-FI-PEG-RGD/DOX at pH = 7 (Figure 30b), an increase in the chemical shift in the peaks (c, e) was detected in the spectrum of G5.NHAc-FI-PEG-RGD/DOX at pH = 5 (Figure 30a). This is because

above pH = 7, all the tertiary amino groups in the PAMAM dendrimer are non-protonated, while below pH = 5, about 70 % of the tertiary amino groups are protonated (*92*).

The protonation of the tertiary amino groups results in an increase in the chemical shift of the adjacent CH_2 groups in the PAMAM dendrimers. Moreover, compared with the ^1H NMR spectrum of DOX·HCl (Figure 30c), the peaks corresponding to the DOX protons show obvious changes after mixing with the G5.NHAc-FI-PEG-RGD dendrimer under both acid and neutral conditions, thereby revealing that intermolecular interactions occur between the dendrimers and the guest molecules. In addition, at pH = 5, line broadening of the DOX proton signals is observed. This can be attributed to a decrease in the degree of freedom of the drug molecules, and also an increase in the ratio of coordinated DOX within the G5.NHAc-FI-PEG-RGD dendrimer.

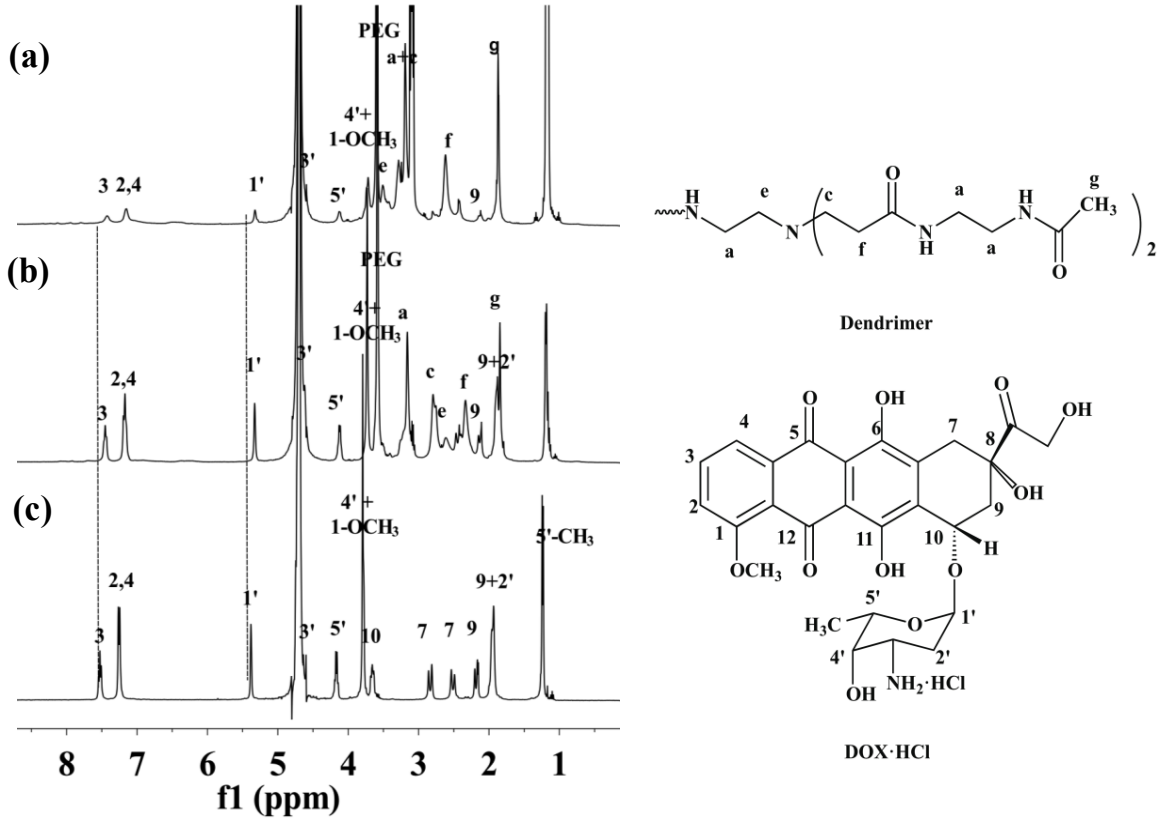

Figure 30 – ^1H NMR spectra of G5.NHAc-FI-PEG-RGD/DOX at pH = 5.0 (a), pH = 7.0 (b), and the free DOX·HCl with self-pH (c). All samples were dissolved in D_2O. The DOX concentration in each prepared sample is 5 mg/mL.

3.4.2 2D NMR SPECTROSCOPY

In order to locate the specific structural units involved in the interaction between G5.NHAc-FI-PEG-RGD and DOX, 2D-NOESY experiments were performed to detect the protons that are spatially close to each other. Figures 31 and 32 show the NOESY spectra of the G5.NHAc-FI-PEG-RGD/DOX complex at pH = 7 and at pH = 5, respectively. The positive sign of the cross-peaks means that the protons involved form part of a slowly tumbling molecule. The presence of these cross peaks indicates that DOX bonds to or is encapsulated within the dendrimer. However, there are no cross-peaks between DOX and the methylene protons found within the interior cavity of the dendrimer. Both DOX and the dendrimer only have cross-peaks between their own protons in the NOESY spectra. Since the phase of the cross-peaks between the DOX protons is the same as that of the diagonal peaks, it may be stated that DOX is incorporated into the G5.NHAc-FI-PEG-RGD dendrimers. In other words, DOX behaves as a part of the macromolecule.

In a previous study (*86*), it was reported that DOX has a reversible interaction with the dendrimer such that both free and coordinated DOX can be found in solution. Since the exchange of DOX between the dendrimer and the solution is fast, on the ^{1}H chemical shift scale, we cannot see separate peaks for DOX that is located within the dendrimer interior and for DOX that is found in the bulk solution. Interestingly, in the NOESY spectrum, strong cross-peaks between the protons of PEG and DOX are evident. These strong cross-peaks are particularly evident in the spectrum of the sample at pH = 7, suggesting a close proximity between the DOX-protons and the PEG-protons of the multifunctional dendrimer. As such, we can conclude that there is stronger hydrogen bonding between PEG ($-OCH_2CH_2$) and non-protonated DOX than between DOX and the interior protons of the dendrimer.

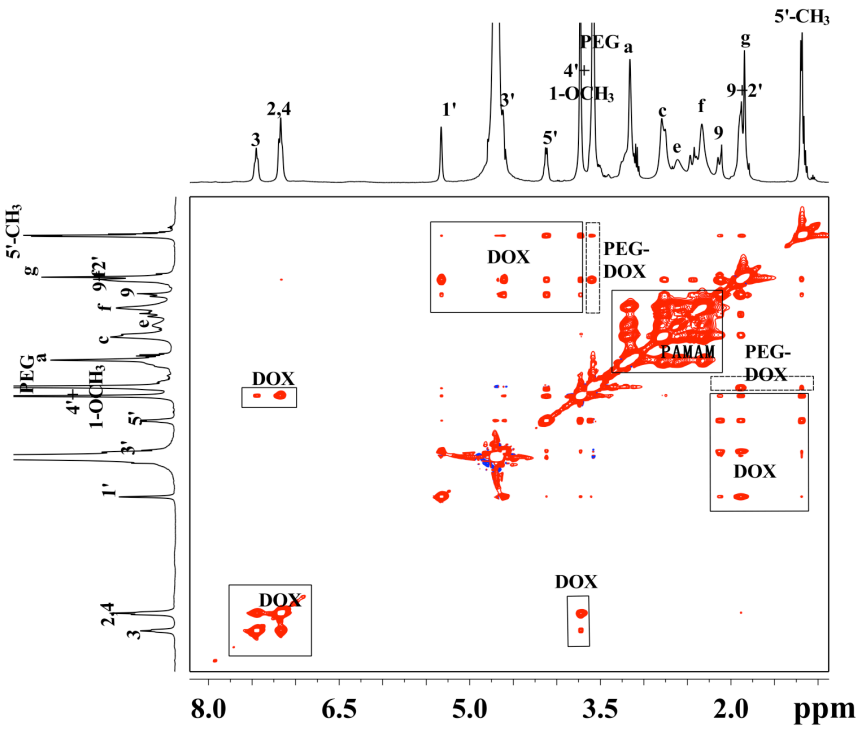

Figure 31 – ^{1}H-^{1}H NOESY spectra of G5.NHAc-FI-PEG-RGD/DOX·HCl/TEA/D_2O at a pH = 7, with a mixing time of 200 ms. The sample was prepared by dissolving 4 mg of the G5.NHAc-FI-PEG-RGD dendrimer in 0.5 mL D_2O, followed by mixing with 2.5 mg DOX·HCl and TEA.

The interaction between G5.NHAc-FI-PEG-RGD and DOX was further investigated by the DOSY technique. DOSY is a NMR-based technique that is able to provide information on the average diffusion coefficients of the components involved in a multicomponent system. The diffusion coefficient reflects the hydrodynamic size and shape of the measured molecule. In this study, the diffusion coefficients of the samples under investigation are listed in Table 3. The average diffusion coefficients (D) measured for DOX in the presence of the G5.NHAc-FI-PEG-RGD dendrimer at pH = 7.0 and at pH = 5.0 were 1.69×10^{-10} m^2/s and 1.39×10^{-10} m^2/s, respectively. These values are much lower than that of free DOX·HCl ($D_{DOX} = 1.96 \times 10^{-10}$ m^2/s). This means that some of the DOX molecules move together with the G5.NHAc-FI-PEG-RGD dendrimers, thereby lowering the average diffusion rate of the formed complexes. The average diffusion coefficient of DOX in the G5.NHAc-FI-PEG-RGD/DOX system at pH = 5.0 is smaller when compared with

that of the G5.NHAc-FI-PEG-RGD/DOX complex prepared at pH = 7.0.

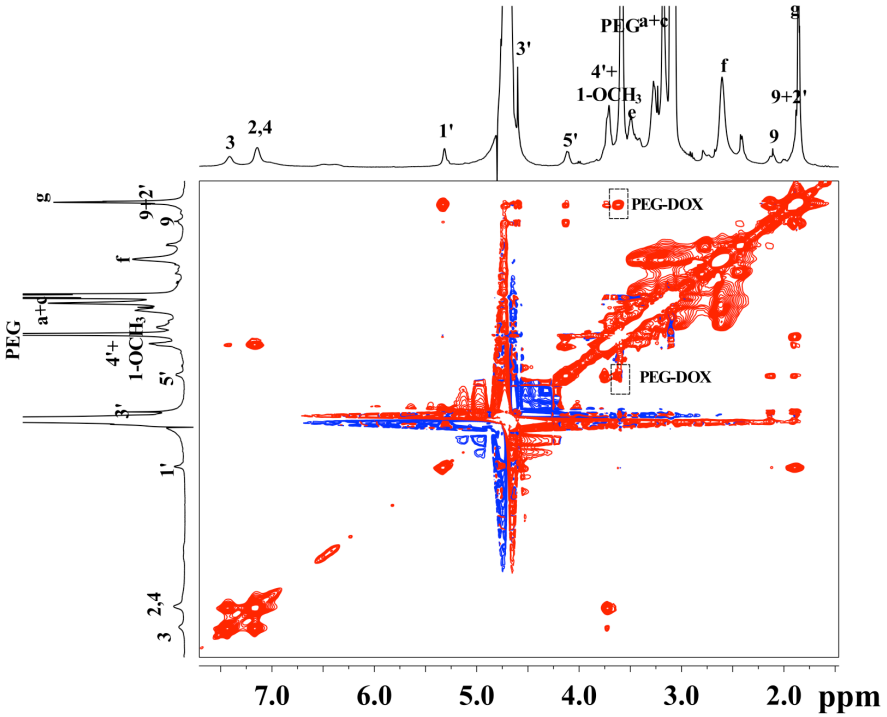

Figure 32 – ^{1}H-^{1}H NOESY spectra of G5.NHAc-FI-PEG-RGD/DOX·HCl/TEA/DCl in D_2O at a pH = 5.0, with a mixing time of 200 ms. The sample was prepared by dissolving 4 mg of the G5.NHAc-FI-PEG-RGD dendrimer in 0.5 mL D_2O, followed by mixing with 2.5 mg DOX·HCl and 2 µL TEA. A 200µl volume of DCl was used to adjust the pH to ~ 5.

This is indicative of a higher number of DOX molecules being complexed with the dendrimer under acidic conditions. Combining the results obtained from the NOESY and DOSY experiments, we can reasonably deduce that during the dendrimer/DOX complex formation, TEA was used to neutralize DOX·HCl, converting it into the hydrophobic DOX drug. In this form, DOX is more compatible with the hydrophobic interior of the dendrimer. The use of DCl to adjust the pH of the aqueous (D_2O) solutions from pH = 7.0 to pH = 5.0 induced the protonation of DOX. This protonation of DOX results in a weakened hydrogen bonding interaction with the PEG moieties that are conjugated to the dendrimer surfaces. Consequently, the

movement of DOX from the interior of the dendrimer towards its surface became slower. This slow release of DOX from the dendrimer interior under acidic conditions can be explained by the stronger dendrimer/DOX interactions and the weaker DOX-PEG interactions that exist.

Table 3 – Diffusion coefficients of samples ($\times 10^{-11}$ m^2/s).

	G5.NHAc-FI-PEG-RGD/DOX complex		G5.NHAc-FI-PEG-RGD	Free DOX·HCl
	Dendrimer	DOX		
pH = 5.0	4.2	13.9	3.9	19.6
pH = 7.0	4.2	16.9	4.2	19.6

3.5 Therapeutic efficacy of DOX encapsulated within G5.NHAc-FI-PEG-RGD dendrimers

The therapeutic efficacy of the DOX encapsulated G5.NHAc-FI-PEG-RGD dendrimers on U87-MG cells was tested using the MTT viability assay (see Figure 33). After incubating the cells with the dendrimer/DOX complexes for 48 h, both free DOX·HCl (5 μM) and G5.NHAc-FI-PEG-RGD/DOX complexes prepared using a DOX concentration of 5 μM were observed to cause a significant loss in cell viability when compared with the control cells that were treated with PBS only ($p < 0.001$ for each). To exclude the possible inherent toxicity of the dendrimers, the multifunctional DOX-free G5.NHAc-FI-PEG-RGD dendrimers were prepared using an equivalent dendrimer concentration and were then tested on the U87-MG cells. It is clear that the G5.NHAc-FI-PEG-RGD dendrimers are non-toxic ($p > 0.05$). These results indicate that the therapeutic activity of the G5.NHAc-FI-PEG-RGD/DOX complexes is solely related to the complexed DOX drug.

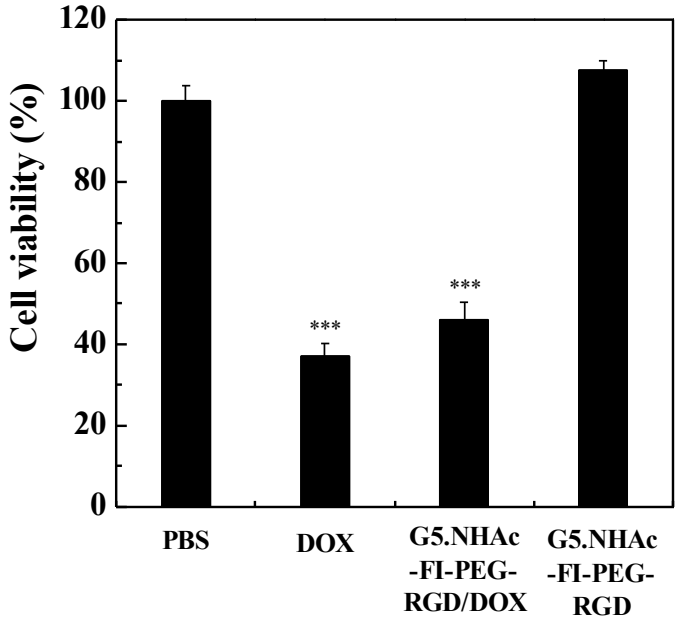

Figure 33 – MTT assay of the viability of the U87-MG cells after treatment with 10 μL PBS buffer (control), free DOX·HCl dissolved in 10 μL PBS (5 μM), G5.NHAc-FI- PEG-RGD/DOX complexes with a DOX concentration of 5 μM, and DOX-free G5.NHAc-FI-PEG-RGD dendrimers prepared using the same dendrimer concentration. The data is expressed as mean ± S.D. (n = 4). Statistical analysis was performed to compare the cell viability upon treatment with PBS, (***) for $p < 0.001$.

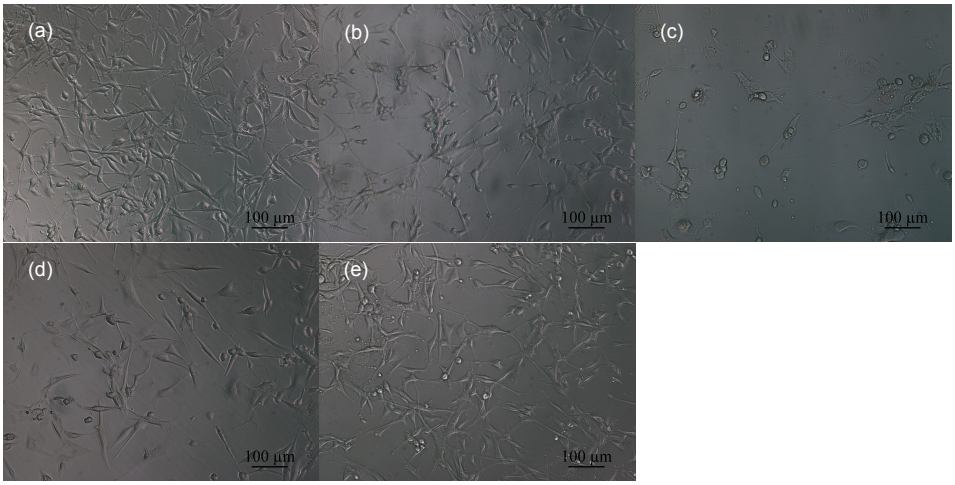

Figure 34 – Photomicrographs of the control U87-MG cells without treatment (a) and the U87-MG cells treated with 10 μL PBS (b), free DOX·HCl (5 μM) (c), DOX (5 μM) complexed with G5.NHAc-FI-PEG-RGD dendrimers (d), and DOX-free G5.NHAc-FI-PEG-RGD dendrimers prepared using the same dendrimer concentration as that used when preparing the G5.NHAc-FI-PEG-RGD/DOX complexes (e).

The cytotoxic effect of the G5.NHAc-FI-PEG-RGD/DOX complexes was further confirmed by the microscopic visualization of the morphology of the U87-MG cells after treatment with the complexes. Figure 34 shows the morphology of the untreated U87-MG cells, as well as the morphology of the cells treated with either PBS buffer, free DOX·HCl, or the G5.NHAc-FI-PEG-RGD/DOX complexes. The U87-MG cells treated either with DOX·HCl in PBS (Figure 34c) or with the G5.NHAc-FI-PEG-RGD/DOX complexes prepared using a similar DOX concentration (Figure 34d) induced comparable morphological changes. Here, a significant portion of the cells became rounded and non-adherent, indicative of cell death. In contrast, no rounded and detached cells were visualized in the control cells that did not undergo DOX treatment (Figure 34a) and in the cells that were treated with only 10 μL PBS (Figure 34b). A similar observation was made for the U87-MG cells that were treated with the DOX-free G5.NHAc-FI-PEG-RGD dendrimers that were prepared using the same dendrimer concentration as that used when preparing the G5.NHAc-FI-PEG-RGD/DOX complexes. It was also found that the multifunctional G5.NHAc-FI-PEG-RGD dendrimers did not induce any prominent morphological modifications in the cells (Figure 34e). This data further suggests that the anticancer activity of the G5.NHAc-FI-PEG-RGD/DOX complexes is solely related to the complexed DOX drug, thereby corroborating the MTT assay results.

3.6 Targeted ability of G5.NHAc-FI-PEG-RGD complexes

The cyclic RGD peptide was selected as a targeting ligand to be conjugated onto the dendrimer surface so as to achieve the specific delivery of DOX to cancer cells overexpressing $\alpha_v\beta_3$ integrins on their membrane surface. The high affinity of $\alpha_v\beta_3$ integrins for RGD peptides is expected to allow the specific binding and internalization of the RGD-modified dendrimers into cancer cells through receptor-mediated endocytosis. U87-MG cells were selected for the specific binding and treatment with the G5.NHAc-FI-PEG-RGD/DOX complexes as these cells overexpress integrins on their membrane surface.

3.6.1 DETERMINATION OF RGD CONCENTRATION FOR BLOCKING INTEGRIN $\alpha_v\beta_3$

In order to test the targeting ability of G5.NHAc-FI-PEG-RGD/DOX, it is important to set up a control group of U87-MG cells in which the $\alpha_v\beta_3$ integrins are inactive. This means that the $\alpha_v\beta_3$ integrins that exist on the U87-MG cell surface must be totally pre-blocked with free RGD peptides before performing the cell internalization experiments.

U87-MG cells were incubated for 1 h at 37 °C with 0.0, 0.5, 1, 2 and 4 μM cyclic RGD. At this stage, G5.NHAc-FI-PEG-RGD dendrimers complexed with 5 μM DOX were added to the pre-treated U87-MG cells for another 4 h at 37 °C. The MTT assay showed cell viability values of 69.7±6.4, 92.2±5.4, 95.8±5.5, 96.5±5.1 and 90.5±2.7 % for the U87-MG cells pre-treated with 0.0, 0.5, 1, 2 and 4 μM cyclic RGD, respectively (see Figure 35). Thus the internalization of the G5.NHAc-FI-PEG-RGD/DOX complexes by the U87-MG cells was, to a considerable extent, effectively inhibited as a result of the $\alpha_v\beta_3$ integrins on the cell surface being blocked by cyclic RGD. It is important to note that, according to the literature, the use of a 2 μM RGD concentration and a 1 h incubation period is sufficient to block the U87-MG cell surface $\alpha_v\beta_3$ integrins (*93*). However, in the present study it was found that complete integrin blocking was achieved when using a lower RGD concentration of 0.5 μM. Nevertheless, a 2 μM RGD concentration was still used in the following studies to block the $\alpha_v\beta_3$ integrins located on the U87-MG cell surface.

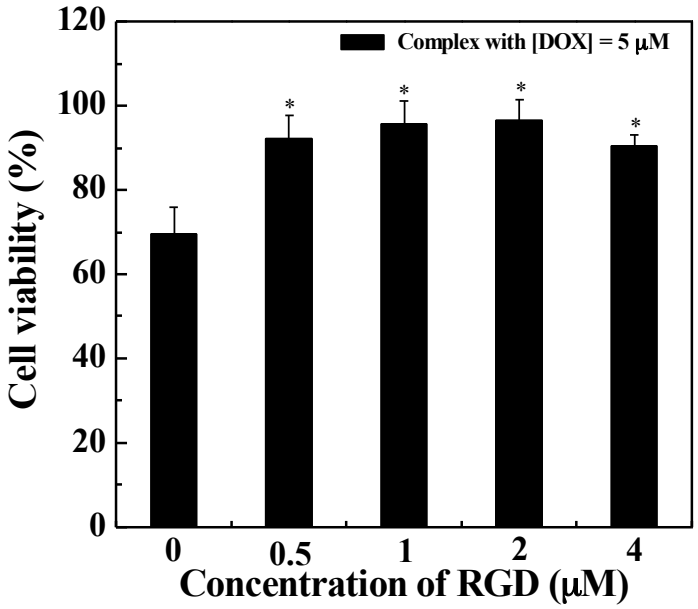

Figure 35 – Cell viability of U87-MG cells pre-treated with 0, 0.5, 1, 2, 4 μM RGD for 1 h and then finally treated with G5.NHAc-FI-PEG-RGD dendrimers complexed with 5 μM DOX. The data is expressed as mean ± S.D. (n = 4). Statistical analysis was performed to compare the cell viability upon treatment with 0 μM RGD, (*) for $p < 0.05$.

3.6.2 CELL UPTAKE OF G5.NHAc-FI-PEG-RGD/DOX

To evaluate the targeting specificity and uptake of the multifunctional RGD-modified G5 dendrimers, comparisons were made between the non-blocked U87-MG cells and the U87-MG cells pre-treated with a 2 μM RGD solution.

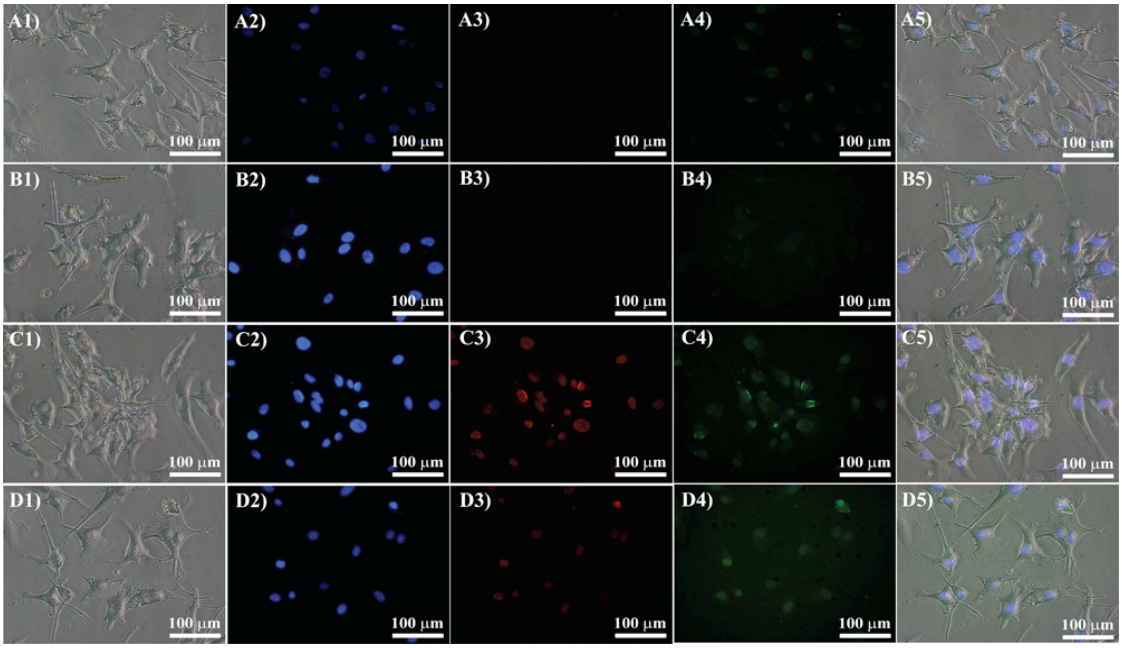

Figure 36 – Fluorescence microscopy images of U87-MG cells treated with EMEM medium A), PBS B), the G5.NHAc-FI-PEG-RGD/DOX complexes only C), and 2 µM RGD for 1 h followed by the G5.NHAc-FI-PEG-RGD/DOX complexes for 4 h D). In all cases, the DOX concentration was kept at 5 µM. For each panel, the images from left to right show the bright field, the blue fluorescence channel detecting the DAPI dye, the red fluorescence channel detecting DOX, the green fluorescence channel detecting the FI, and the merged images of the above three modes. All the images were collected under the equivalent instrumental conditions.

The conjugation of the FI moiety onto the G5 dendrimers enables the fluorescence microscopic imaging of the cellular uptake of the G5.NHAc-FI-PEG-RGD/DOX complexes into the U87-MG cells. Figure 36 shows that after 4 h incubation of the U87-MG cells with the G5.NHAc-FI-PEG-RGD/DOX complexes, only the cells that did not undergo pre-blocking with free RGD showed significant red and green fluorescence signals. These signals are associated with the specific internalization of the G5.NHAc-FI-PEG-RGD/DOX complexes into the cytoplasm of the cells (Figure 36 (C3-4)). The green (Figure 36 (C4)) and the red (Figure 36 (C3)) fluorescence signals are indicative that both the FI-labeled dendrimer

and the complexed DOX were internalized by the U87-MG cells. The slightly purple signals evident in the merged images in Figure 36 (C5) further demonstrate this phenomenon. In comparison, under similar microscopic conditions, the U87-MG cells that were pre-blocked with free RGD and that were treated with the same complexes showed less intense red and green fluorescence signals (Figure 36 (D3-4)). Overall, the results combined suggest that the G5.NHAc-FI-PEG-RGD dendrimers display an important targeting ability.

3.6.3 MTT ASSAY TO TEST THE TARGETING INHIBITION OF G5.NHAc-FI-PEG-RGD/DOX

To prove that the G5.NHAc-FI-PEG-RGD/DOX complexes were able to specifically inhibit U87-MG cells, the cells were incubated with the complexes for 4 h. The medium in each well was then replaced with the same volume of fresh medium and incubated for a further 48 h at 37 °C. At this stage, the MTT assay was performed to assess the viability of the cells. Figure 37 shows the viability of the U87-MG cells after treatment with 10 µL of either PBS buffer (control), the G5.NHAc-FI-PEG-RGD/DOX complex (DOX concentration of 5 µM) without integrin pre-blocking or the G5.NHAc-FI-PEG-RGD/DOX complex (DOX concentration of 5 µM) with integrin pre-blocking for 1h. Under each condition, the cell viability values recorded were 100.0±5.0, 69.7±6.4 and 96.5±5.1 %, respectively. It can be seen that the treatment of the U87-MG cells with the G5.NHAc-FI-PEG-RGD/DOX complexes resulted in a significant decrease in the cell viability ($p < 0.01$ versus control). In contrast, RGD pre-blocking of the U87-MG cells led to 96.5% viability. From this experiment it is evident that the G5.NHAc-FI-PEG-RGD/DOX complexes provided a targeted inhibition of the cancer cells *via* RGD receptor-mediated binding and intracellular uptake.

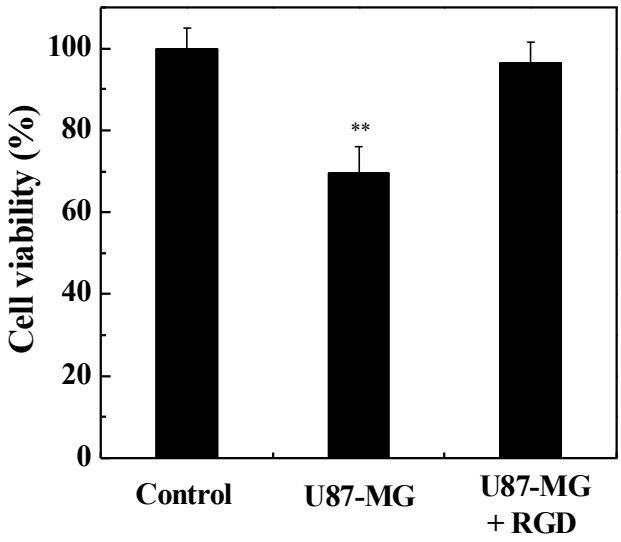

Figure 37 – MTT viability assay of the U87-MG cells after 4 h treatment with either 10 μL PBS or with the G5.NHAc-FI-PEG-RGD/DOX complexes (DOX concentration of 5 μM) prepared with and without integrin pre-blocking using a 2 μM RGD solution for 1 h. After incubating the U87-MG cells with the dendrimer/DOX complexes for 48h, the MTT assay was performed. The data is expressed as mean ± S.D. (n = 4). Statistical analysis was performed to compare the cell viability upon treatment with PBS buffer, (**) for $p < 0.01$.

3.6.4 DOSAGE OF G5.NHAc-FI-PEG-RGD/DOX & CELL VIABILITY

In this study, U87-MG cells were first pretreated with serum free EMEM or with 2 μM RGD for 1h. The U87-MG cells were then incubated for an additional 4 h at 37°C following the treatment of the cells with G5.NHAc-FI-PEG-RGD/DOX complexes prepared taking into account DOX concentrations of 1.25, 2.5, 5, 10 and 20 μM. The cell viability of the U87-MG cells after treatment with the G5.NHAc-FI-PEG-RGD/DOX complexes was 76.8±5.2, 82.7±14.2, 71.9±6.5, 64.8±9.2, and 57.4±4.2 % for RGD = 0 μM; and 98.8±4.1, 83.7±7.2, 86.3±12.9, 73.9±6.0 and 67.9±8.5 % for RGD = 2 μM, respectively (see Figure 38). From the MTT assay results recorded in Figure 32, it was found that a higher concentration of DOX led to lower values of cell viability in the U87-MG cells.

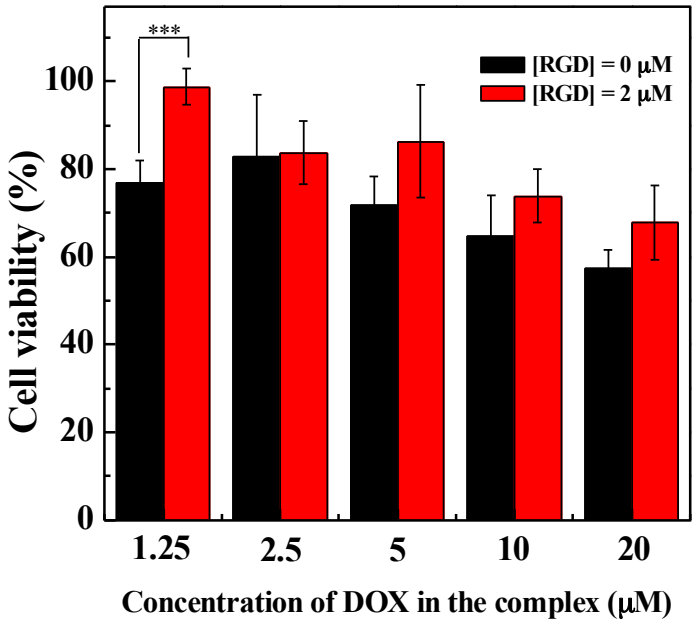

Figure 38 – Cell viability of the U87-MG cells treated with 0 μM RGD (black) or with 2 μM RGD (red) for 1 h. The cells were then treated for an additional 4 h with G5.NHAc-FI-PEG-RGD/DOX complexes prepared taking into account DOX concentrations of 1.25, 2.5, 5, 10, 20 μM . The data is expressed as mean ± S.D. (n = 4). Statistical analysis was performed to compare the cell viability between the U87-MG cells that underwent treatment with or without RGD under the same concentration of DOX, (***) for $p < 0.001$.

3.6.5 INCUBATION TIME & CELL VIABILITY

In this study, the G5.NHAc-FI-PEG-RGD dendrimer was complexed with 5 μM DOX. The prepared complexes were then placed in contact with the U87-MG cells for 0, 1, 2, 4 and 6.5 h in serum-containing medium. The results obtained using the MTT assay showed that the viability of the U87-MG cells decreased with longer incubation times (see Figure 39).

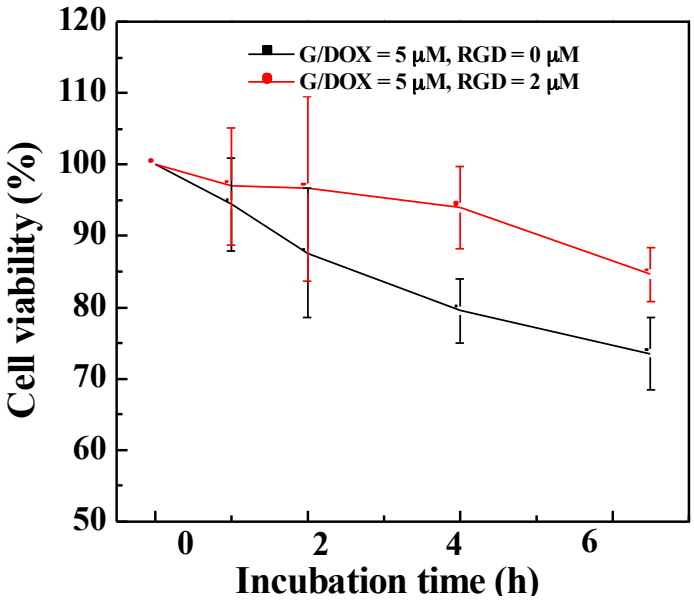

Figure 39 – Cell viability of the U87-MG cells treated with the G5.NHAc-FI-PEG-RGD/DOX complexes using different incubation times.

CHAPTER 4 – GENERAL CONCLUSION

CHAPTER 4 – GENERAL CONCLUSIONS

In summary, multifunctional FI-, PEG-, RGD- modified G5 dendrimers (G5.NHAc-FI-PEG-RGD) were synthesized, and successfully loaded with the antitumor agent, DOX. The formed G5.NHAc-FI-PEG-RGD/DOX complexes were stable and displayed a sustained drug release profile. Importantly, the formed G5.NHAc-FI-PEG-RGD/DOX complexes were able to specifically target U87-MG cells that overexpress $\alpha_v\beta_3$ integrins and displayed specific toxicity towards these cells. Moreover, the results demonstrated a good correlation between the NMR studies (host/guest interactions) and the release profile of the drug. Overall, this study provided valuable knowledge for the design of other different multifunctional dendrimer-based drug carrier systems that may even be considered beyond anticancer applications.

REFERENCES

1. Wang, Y.; Guo, R.; Cao, X. Encapsulation of 2-Methoxyestradiol within Multifunctional Poly(Amidoamine) Dendrimers for Targeted Cancer Therapy. *Biomaterials* **2011,** *32*, 3322-3329.
2. Panyam, J.; Labhasetwar, V. Biodegradable Nanoparticles for Drug and Gene Delivery to Cells and Tissue. *Adv. Drug Deliv. Rev.* **2003,** *55*, 329-347.
3. Medley, C.D.; Smith, J.E.; Tang, Z. Gold Nanoparticle-Based Colorimetric Assay for the Direct Detection of Cancerous Cells. *Anal. Chem.* **2008,** *80*, 1067-1072.
4. Brambilla, D.; Nicolas, J.; Le Droumaguet, B. Design of Fluorescently Tagged Poly(Alkyl Cyanoacrylate) Nanoparticles for Human Brain Endothelial Cell Imaging. *Chem. Commun.* **2010,** *46*, 2602-2604.
5. Vauthier, C.; Dubernet, C.; Chauvierre, C. Drug Delivery to Resistant Tumors: The Potential of Poly(Alkyl Cyanoacrylate) Nanoparticles. *J. Control. Release* **2003,** *93*, 151-160.
6. Yih, T.; Al-Fandi, M. Engineered Nanoparticles as Precise Drug Delivery Systems. *J. Cell. Biochem.* **2006,** *97*, 1184-1190.
7. Bose, S.; Tarafder, S. Calcium Phosphate Ceramic Systems in Growth Factor and Drug Delivery for Bone Tissue Engineering: A Review. *Acta Biomater.* **2012,** *8*, 1401-1421.
8. Arruebo, M.; Fernández-Pacheco, R.; Ibarra, M.R. Magnetic Nanoparticles for

Drug Delivery. *Nano Today* **2007,** *2*, 22-32.

9. Kumari, A.; Yadav, S.K.; Yadav, S.C. Biodegradable Polymeric Nanoparticles Based Drug Delivery Systems. *Colloid Surf. B-Biointerfaces* **2010,** *75*, 1-18.

10. Gillies, E.R.; Frechet, J.M. Dendrimers and Dendritic Polymers in Drug Delivery. *Drug Discov. Today* **2005,** *10*, 35-43.

11. Parveen, S.; Misra, R.; Sahoo, S.K. Nanoparticles: A Boon to Drug Delivery, Therapeutics, Diagnostics and Imaging. *Nanomed.-Nanotechnol. Biol. Med.* **2012,** *8*, 147-166.

12. Islam, M.T.; Majoros, I.J.; Baker Jr, J.R. HPLC Analysis of PAMAM Dendrimer Based Multifunctional Devices. *J. Chromatogr. B* **2005,** *822*, 21-26.

13. Peer, D.; Karp, J.M.; Hong, S. Nanocarriers as an Emerging Platform for Cancer Therapy. *Nat. Nanotechnol.* **2007,** *2*, 751-760.

14. Daftarian, P.; Kaifer, A.E.; Li, W. Peptide-Conjugated PAMAM Dendrimer as a Universal DNA Vaccine Platform to Target Antigen-Presenting Cells. *Cancer Res.* **2011,** *71*, 7452-7462.

15. Tomalia, D.; Reyna, L.; Svenson, S. Dendrimers as Multi-Purpose Nanodevices for Oncology Drug Delivery and Diagnostic Imaging. *Biochem. Soc. Trans.* **2007,** *35*, 61-67.

16. Majoros, I.J.; Thomas, T.P.; Mehta, C.B. Poly(Amidoamine) Dendrimer-Based Multifunctional Engineered Nanodevice for Cancer Therapy. *J. Med. Chem.* **2005,** *48*, 5892-5899.

17. Morgan, M.T.; Carnahan, M.A.; Immoos, C.E. Dendritic Molecular Capsules for Hydrophobic Compounds. *J. Am. Chem. Soc.* **2003,** *125*, 15485-15489.

18. Morgan, M.T.; Nakanishi, Y.; Kroll, D.J. Dendrimer-Encapsulated Camptothecins: Increased Solubility, Cellular Uptake, and Cellular Retention Affords Enhanced Anticancer Activity in Vitro. *Cancer Res.* **2006,** *66*, 11913-11921.

19. Dhanikula, R.S.; Argaw, A.; Bouchard, J.-F. Methotrexate Loaded Polyether-Copolyester Dendrimers for the Treatment of Gliomas: Enhanced Efficacy and Intratumoral Transport Capability. *Mol. Pharm.* **2008,** *5*, 105-116.

20. Wang, Y.; Cao, X.; Guo, R. Targeted Delivery of Doxorubicin into Cancer Cells Using a Folic Acid–Dendrimer Conjugate. *Polym. Chem.* **2011,** *2*, 1754-1760.

21. Shi, X.; Wang, S.; Meshinchi, S. Dendrimer-Entrapped Gold Nanoparticles as a Platform for Cancer-Cell Targeting and Imaging. *Small* **2007,** *3*, 1245-1252.

22. Majoros, I.J.; Myc, A.; Thomas, T. PAMAM Dendrimer-Based Multifunctional Conjugate for Cancer Therapy: Synthesis, Characterization, and Functionality. *Biomacromolecules* **2006,** *7*, 572-579.

23. Liu, H.; Xu, Y.; Wen, S. Targeted Tumor Computed Tomography Imaging Using Low-Generation Dendrimer-Stabilized Gold Nanoparticles. *Chem.-Eur. J.* **2013,** *19*, 6409-6416.

24. Shi, X.; Wang, S.H.; Shen, M. Multifunctional Dendrimer-Modified

Multiwalled Carbon Nanotubes: Synthesis, Characterization, and *in Vitro* Cancer Cell Targeting and Imaging. *Biomacromolecules* **2009,** *10*, 1744-1750.

25. Shen, M.; Sun, K.; Shi, X. Hydroxylated Dendrimer-Stabilized Gold and Silver Nanoparticles: Spontaneous Formation, Characterization, and Surface Properties. *Curr. Nanosci.* **2010,** *6*, 307-314.

26. Shi, X.; Thomas, T.P.; Myc, L.A. Synthesis, Characterization, and Intracellular Uptake of Carboxyl-Terminated Poly(Amidoamine) Dendrimer-Stabilized Iron Oxide Nanoparticles. *Phys. Chem. Chem. Phys.* **2007,** *9*, 5712-5720.

27. Peng, C.; Zheng, L.; Chen, Q. PEGylated Dendrimer-Entrapped Gold Nanoparticles for *in Vivo* Blood Pool and Tumor Imaging by Computed Tomography. *Biomaterials* **2012,** *33*, 1107-1119.

28. Chen, H.-T.; Neerman, M.F.; Parrish, A.R. Cytotoxicity, Hemolysis, and Acute *in Vivo* Toxicity of Dendrimers Based on Melamine, Candidate Vehicles for Drug Delivery. *J. Am. Chem. Soc.* **2004,** *126*, 10044-10048.

29. Kim, Y.; Klutz, A.M.; Jacobson, K.A. Systematic Investigation of Polyamidoamine Dendrimers Surface-Modified with Poly(Ethylene Glycol) for Drug Delivery Applications: Synthesis, Characterization, and Evaluation of Cytotoxicity. *Bioconjugate Chem.* **2008,** *19*, 1660-1672.

30. Mignani, S.; El Kazzouli, S.; Bousmina, M. Expand Classical Drug Administration Ways by Emerging Routes Using Dendrimer Drug Delivery Systems: A Concise Overview. *Adv. Drug Deliv. Rev.* **2013,** *65*, 1316–1330.

31. Esfand, R.; Tomalia, D.A. Poly(Amidoamine) (PAMAM) Dendrimers: From Biomimicry to Drug Delivery and Biomedical Applications. *Drug Discov. Today* **2001,** *6*, 427-436.

32. Gordon, A.N.; Fleagle, J.T.; Guthrie, D. Recurrent Epithelial Ovarian Carcinoma: A Randomized Phase III Study of Pegylated Liposomal Doxorubicin Versus Topotecan. *J. Clin. Oncol.* **2001,** *19*, 3312-3322.

33. Lamm, D.L.; Blumenstein, B.A.; Crawford, E.D. A Randomized Trial of Intravesical Doxorubicin and Immunotherapy with Bacille Calmette–Guerin for Transitional-Cell Carcinoma of the Bladder. *N. Engl. J. Med.* **1991,** *325*, 1205-1209.

34. Santoro, A.; Tursz, T.; Mouridsen, H. Doxorubicin Versus Cyvadic Versus Doxorubicin Plus Ifosfamide in First-Line Treatment of Advanced Soft Tissue Sarcomas: A Randomized Study of the European Organization for Research and Treatment of Cancer Soft Tissue and Bone Sarcoma Group. *J. Clin. Oncol.* **1995,** *13*, 1537-1545.

35. Zhu, S.; Hong, M.; Zhang, L. PEGylated PAMAM Dendrimer-Doxorubicin Conjugates: *In Vitro* Evaluation and *in Vivo* Tumor Accumulation. *Pharm. Res.* **2010,** *27*, 161-174.

36. Papagiannaros, A.; Dimas, K.; Papaioannou, G.T. Doxorubicin–PAMAM Dendrimer Complex Attached to Liposomes: Cytotoxic Studies against Human Cancer Cell Lines. *Int. J. Pharm.* **2005,** *302*, 29-38.

37. Zhu, J.; Shi, X. Dendrimer-Based Nanodevices for Targeted Drug Delivery

Applications. *J. Mater. Chem. B* **2013,** *1*, 4199-4211.

38. Guo, R.; Shi, X. Dendrimers in Cancer Therapeutics and Diagnosis. *Curr. Drug Metab.* **2012,** *13*, 1097-1109.

39. Jansen, J.F.; Meijer, E.; de Brabander-van den Berg, E.M. The Dendritic Box: Shape-Selective Liberation of Encapsulated Guests. *J. Am. Chem. Soc.* **1995,** *117*, 4417-4418.

40. D'Emanuele, A.; Attwood, D. Dendrimer–Drug Interactions. *Adv. Drug Deliv. Rev.* **2005,** *57*, 2147-2162.

41. Kurtoglu, Y.E.; Mishra, M.K.; Kannan, S. Drug Release Characteristics of PAMAM Dendrimer–Drug Conjugates with Different Linkers. *Int. J. Pharm.* **2010,** *384*, 189-194.

42. Fleige, E.; Quadir, M.A.; Haag, R. Stimuli-Responsive Polymeric Nanocarriers for the Controlled Transport of Active Compounds: Concepts and Applications. *Adv. Drug Deliv. Rev.* **2012,** *64*, 866-884.

43. Yuan, H.; Luo, K.; Lai, Y. A Novel Poly(L-Glutamic Acid) Dendrimer Based Drug Delivery System with Both pH-Sensitive and Targeting Functions. *Mol. Pharm.* **2010,** *7*, 953-962.

44. Choi, S.K.; Thomas, T.; Li, M.-H. Light-Controlled Release of Caged Doxorubicin from Folate Receptor-Targeting PAMAM Dendrimer Nanoconjugate. *Chem. Commun.* **2010,** *46*, 2632-2634.

45. Maeda, H.; Wu, J.; Sawa, T. Tumor Vascular Permeability and the EPR Effect in Macromolecular Therapeutics: A Review. *J. Control. Release* **2000,** *65*,

271-284.

46. Patri, A.K.; Kukowska-Latallo, J.F.; Baker Jr, J.R. Targeted Drug Delivery with Dendrimers: Comparison of the Release Kinetics of Covalently Conjugated Drug and Non-Covalent Drug Inclusion Complex. *Adv. Drug Deliv. Rev.* **2005,** *57*, 2203-2214.

47. Jaracz, S.; Chen, J.; Kuznetsova, L.V. Recent Advances in Tumor-Targeting Anticancer Drug Conjugates. *Bioorg. Med. Chem.* **2005,** *13*, 5043-5054.

48. Han, M.; Lv, Q.; Tang, X.-J. Overcoming Drug Resistance of MCF-7/ADR Cells by Altering Intracellular Distribution of Doxorubicin Via MVP Knockdown with a Novel Sirna Polyamidoamine-Hyaluronic Acid Complex. *J. Control. Release* **2012,** *163*, 136-144.

49. Barth, R.F.; Adams, D.M.; Soloway, A.H. Boronated Starburst Dendrimer-Monoclonal Antibody Immunoconjugates: Evaluation as a Potential Delivery System for Neutron Capture Therapy. *Bioconjugate Chem.* **1994,** *5*, 58-66.

50. Han, L.; Huang, R.; Li, J. Plasmid pORF-hTRAIL and Doxorubicin Co-Delivery Targeting to Tumor Using Peptide-Conjugated Polyamidoamine Dendrimer. *Biomaterials* **2011,** *32*, 1242-1252.

51. Dijkgraaf, I.; Rijnders, A.Y.; Soede, A. Synthesis of DOTA-Conjugated Multivalent Cyclic-RGD Peptide Dendrimers Via 1, 3-Dipolar Cycloaddition and Their Biological Evaluation: Implications for Tumor Targeting and Tumor Imaging Purposes. *Org. Biomol. Chem.* **2007,** *5*, 935-944.

52. Antony, A.C. Folate Receptors. *Annu. Rev. Nutr.* **1996,** *16*, 501-521.

53. Garin-Chesa, P.; Campbell, I.; Saigo, P. Trophoblast and Ovarian Cancer Antigen Lk26. Sensitivity and Specificity in Immunopathology and Molecular Identification as a Folate-Binding Protein. *Am. J. Pathol.* **1993,** *142*, 557-567.

54. Weitman, S.D.; Lark, R.H.; Coney, L.R. Distribution of the Folate Receptor GP38 in Normal and Malignant Cell Lines and Tissues. *Cancer Res.* **1992,** *52*, 3396-3401.

55. Hong, S.; Leroueil, P.R.; Majoros, I.J. The Binding Avidity of a Nanoparticle-Based Multivalent Targeted Drug Delivery Platform. *Chem. Biol.* **2007,** *14*, 107-115.

56. Sudimack, J.; Lee, R.J. Targeted Drug Delivery Via the Folate Receptor. *Adv. Drug Deliv. Rev.* **2000,** *41*, 147-162.

57. Luo, Y.; Ziebell, M.R.; Prestwich, G.D. A Hyaluronic Acid-Taxol Antitumor Bioconjugate Targeted to Cancer Cells. *Biomacromolecules* **2000,** *1*, 208-218.

58. Turley, E.A.; Belch, A.J.; Poppema, S. Expression and Function of a Receptor for Hyaluronan-Mediated Motility on Normal and Malignant B Lymphocytes. *Blood* **1993,** *81*, 446-453.

59. Rudzki, Z.; Jothy, S. CD44 and the Adhesion of Neoplastic Cells. *J. Clin. Pathol.* **1997,** *50*, 57-71.

60. Lesley, J.; Hyman, R.; English, N. CD44 in Inflammation and Metastasis. *Glycoconjugate J.* **1997,** *14*, 611-622.

61. Entwistle, J.; Hall, C.L.; Turley, E.A. HA Receptors: Regulators of Signalling

to the Cytoskeleton. *J. Cell. Biochem.* **1996,** *61*, 569-577.

62. Coradini, D.; Pellizzaro, C.; Miglierini, G. Hyaluronic Acid as Drug Delivery for Sodium Butyrate: Improvement of the Anti-Proliferative Activity on a Breast-Cancer Cell Line. *Int. J. Cancer* **1999,** *81*, 411-416.

63. Lee, H.; Lee, K.; Park, T.G. Hyaluronic Acid− Paclitaxel Conjugate Micelles: Synthesis, Characterization, and Antitumor Activity. *Bioconjugate Chem.* **2008,** *19*, 1319-1325.

64. Yadav, A.K.; Mishra, P.; Mishra, A.K. Development and Characterization of Hyaluronic Acid–Anchored PLGA Nanoparticulate Carriers of Doxorubicin. *Nanomed.-Nanotechnol. Biol. Med.* **2007,** *3*, 246-257.

65. Ojima, I.; Geng, X.; Wu, X. Tumor-Specific Novel Taxoid-Monoclonal Antibody Conjugates. *J. Med. Chem.* **2002,** *45*, 5620-5623.

66. Chari, R.V. Targeted Delivery of Chemotherapeutics: Tumor-Activated Prodrug Therapy. *Adv. Drug Deliv. Rev.* **1998,** *31*, 89-104.

67. Hamann, P.R.; Hinman, L.M.; Hollander, I. Gemtuzumab Ozogamicin, a Potent and Selective Anti-CD33 Antibody-Calicheamicin Conjugate for Treatment of Acute Myeloid Leukemia. *Bioconjugate Chem.* **2002,** *13*, 47-58.

68. Senter, P.D. Potent Antibody Drug Conjugates for Cancer Therapy. *Curr. Opin. Chem. Biol.* **2009,** *13*, 235-244.

69. Boger, D.L.; Johnson, D.S. Cc-1065 and the Duocarmycins: Understanding Their Biological Function through Mechanistic Studies. *Angew. Chem.-Int. Edit.* **1996,** *35*, 1438-1474.

70. Doronina, S.O.; Toki, B.E.; Torgov, M.Y. Development of Potent Monoclonal Antibody Auristatin Conjugates for Cancer Therapy. *Nat. Biotechnol.* **2003,** *21*, 778-784.

71. Ahmad, I.; Longenecker, M.; Samuel, J. Antibody-Targeted Delivery of Doxorubicin Entrapped in Sterically Stabilized Liposomes Can Eradicate Lung Cancer in Mice. *Cancer Res.* **1993,** *53*, 1484-1488.

72. Kaneko, T.; Willner, D.; Monkovic, I. New Hydrazone Derivatives of Adriamycin and Their Immunoconjugates-a Correlation between Acid Stability and Cytotoxicity. *Bioconjugate Chem.* **1991,** *2*, 133-141.

73. Doronina, S.O.; Mendelsohn, B.A.; Bovee, T.D. Enhanced Activity of Monomethylauristatin F through Monoclonal Antibody Delivery: Effects of Linker Technology on Efficacy and Toxicity. *Bioconjugate Chem.* **2006,** *17*, 114-124.

74. Hansson, Y.; Paulie, S.; Ben-Aissa, H. Radioimmunolocalisation of Bladder Tumors Xenotransplanted in Nude Mice. *Anticancer Res.* **1987,** *8*, 435-441.

75. Guo, R.; Yao, Y.; Cheng, G. Synthesis of Glycoconjugated Poly(Amindoamine) Dendrimers for Targeting Human Liver Cancer Cells. *RSC Adv.* **2012,** *2*, 99-102.

76. Bhadra, D.; Yadav, A.; Bhadra, S. Glycodendrimeric Nanoparticulate Carriers of Primaquine Phosphate for Liver Targeting. *Int. J. Pharm.* **2005,** *295*, 221-233.

77. Hill, E.; Shukla, R.; Park, S.S. Synthetic PAMAM–RGD Conjugates Target

and Bind to Odontoblast-Like MDPC 23 Cells and the Predentin in Tooth Organ Cultures. *Bioconjugate Chem.* **2007,** *18*, 1756-1762.

78. Schally, A.V.; Nagy, A. Cancer Chemotherapy Based on Targeting of Cytotoxic Peptide Conjugates to Their Receptors on Tumors. *Eur. J. Endocrinol.* **1999,** *141*, 1-14.

79. Kiaris, H.; Schally, A.; Nagy, A. Targeted Cytotoxic Analogue of Bombesin/Gastrin-Releasing Peptide Inhibits the Growth of H-69 Human Small-Cell Lung Carcinoma in Nude Mice. *Br. J. Cancer* **1999,** *81*, 966.

80. Chen, K.; Chen, X. Integrin Targeted Delivery of Chemotherapeutics. *Theranostics* **2011,** *1*, 189-200.

81. Li, Z.; Huang, P.; Zhang, X. RGD-Conjugated Dendrimer-Modified Gold Nanorods for *in Vivo* Tumor Targeting and Photothermal Therapy. *Mol. Pharm.* **2009,** *7*, 94-104.

82. Shukla, R.; Thomas, T.P.; Peters, J. Tumor Angiogenic Vasculature Targeting with Pamam Dendrimer–Rgd Conjugates. *Chem. Commun.* **2005,** 5739-5741.

83. Zhu, S.; Qian, L.; Hong, M. Rgd-Modified PEG-PAMAM-DOX Conjugate: *In Vitro* and *in Vivo* Targeting to Both Tumor Neovascular Endothelial Cells and Tumor Cells. *Adv. Mater.* **2011,** *23*, H84-H89.

84. Li, Z.; Huang, P.; Zhang, X. RGD-Conjugated Dendrimer-Modified Gold Nanorods for *in Vivo* Tumor Targeting and Photothermal Therapy. *Mol. Pharm.* **2009,** *7*, 94-104.

85. Hu, J.; Cheng, Y.; Wu, Q. Host−Guest Chemistry of Dendrimer-Drug

Complexes. 2. Effects of Molecular Properties of Guests and Surface Functionalities of Dendrimers. *J. Phys. Chem. B* **2009,** *113*, 10650-10659.

86. Zhang, M.; Guo, R.; Kéri, M. Impact of Dendrimer Surface Functional Groups on the Release of Doxorubicin from Dendrimer Carriers. *J. Phys. Chem. B* **2014,** *118*, 1696–1706.

87. Pandita, D.; Santos, J.L.; Rodrigues, J. Gene Delivery into Mesenchymal Stem Cells: A Biomimetic Approach Using RGD Nanoclusters Based on Poly(Amidoamine) Dendrimers. *Biomacromolecules* **2011,** *12*, 472-481.

88. Santos, J.L.; Oliveira, H.; Pandita, D. Functionalization of Poly(Amidoamine) Dendrimers with Hydrophobic Chains for Improved Gene Delivery in Mesenchymal Stem Cells. *J. Control. Release* **2010,** *144*, 55-64.

89. Nasongkla, N.; Shuai, X.; Ai, H. cRGD-Functionalized Polymer Micelles for Targeted Doxorubicin Delivery. *Angew. Chem.-Int. Edit.* **2004,** *116*, 6483-6487.

90. Liao, H.; Liu, H.; Li, Y. Antitumor Efficacy of Doxorubicin Encapsulated within PEGylated Poly(Amidoamine) Dendrimers. *J. Appl. Polym. Sci.* **2014,** *131*, 40358.

91. Cakara, D.; Kleimann, J.; Borkovec, M. Microscopic Protonation Equilibria of Poly(Amidoamine) Dendrimers from Macroscopic Titrations. *Macromolecules* **2003,** *36*, 4201-4207.

92. Chen, W.; Tomalia, D.A.; Thomas, J.L. Unusual pH-Dependent Polarity Changes in PAMAM Dendrimers: Evidence for pH-Responsive

Conformational Changes. *Macromolecules* **2000,** *33*, 9169-9172.

93. Cheng, S.-H.; Lee, C.-H.; Chen, M.-C. Tri-Functionalization of Mesoporous Silica Nanoparticles for Comprehensive Cancer Theranostics-the Trio of Imaging, Targeting and Therapy. *J. Mater. Chem.* **2010,** *20*, 6149-6157.

ANNEX

ANNEX I – ^{1}H NMR spectra of starting materials

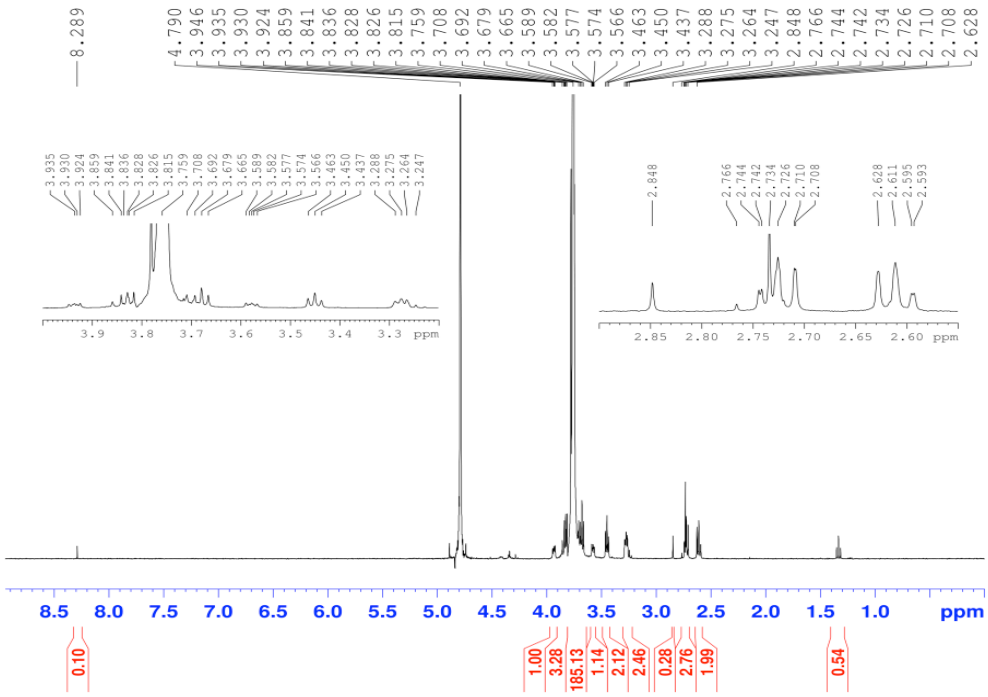

Figure 40 – ^{1}H NMR of HOOC-PEG-NH_2 in D_2O

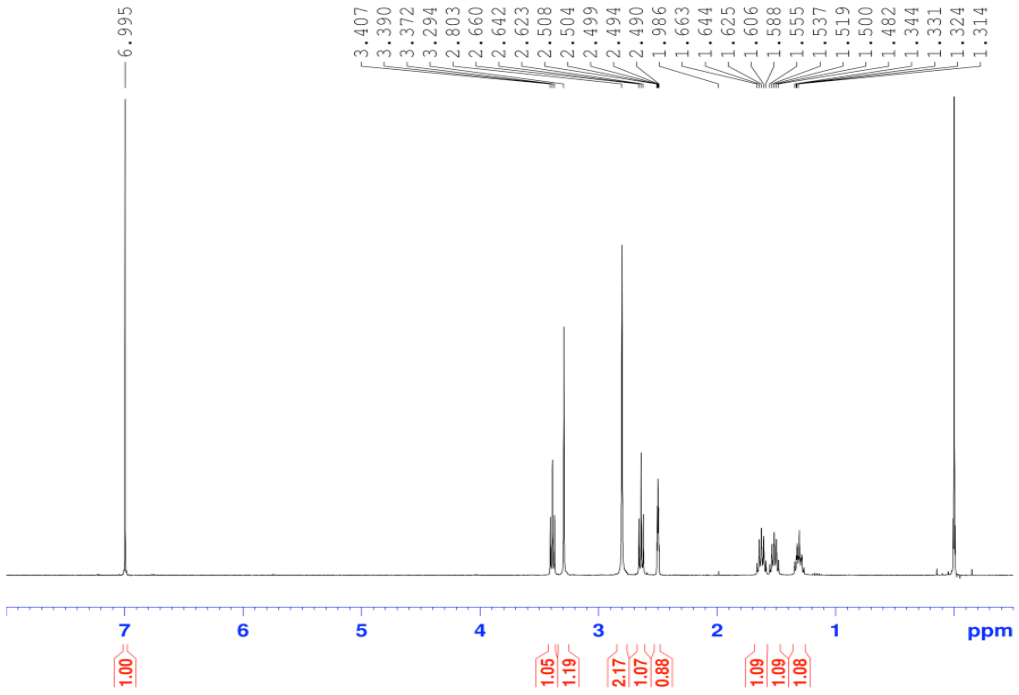

Figure 41 – ^{1}H NMR of MHS in D_2O.

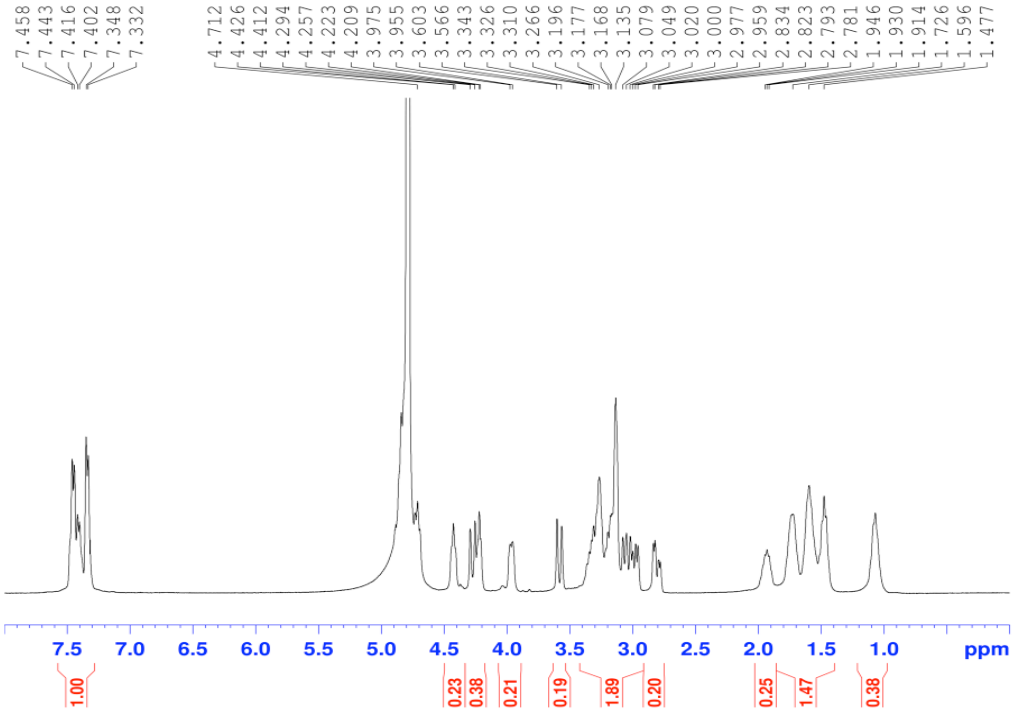

Figure 42 – ^{1}H NMR of RGD in D_2O.

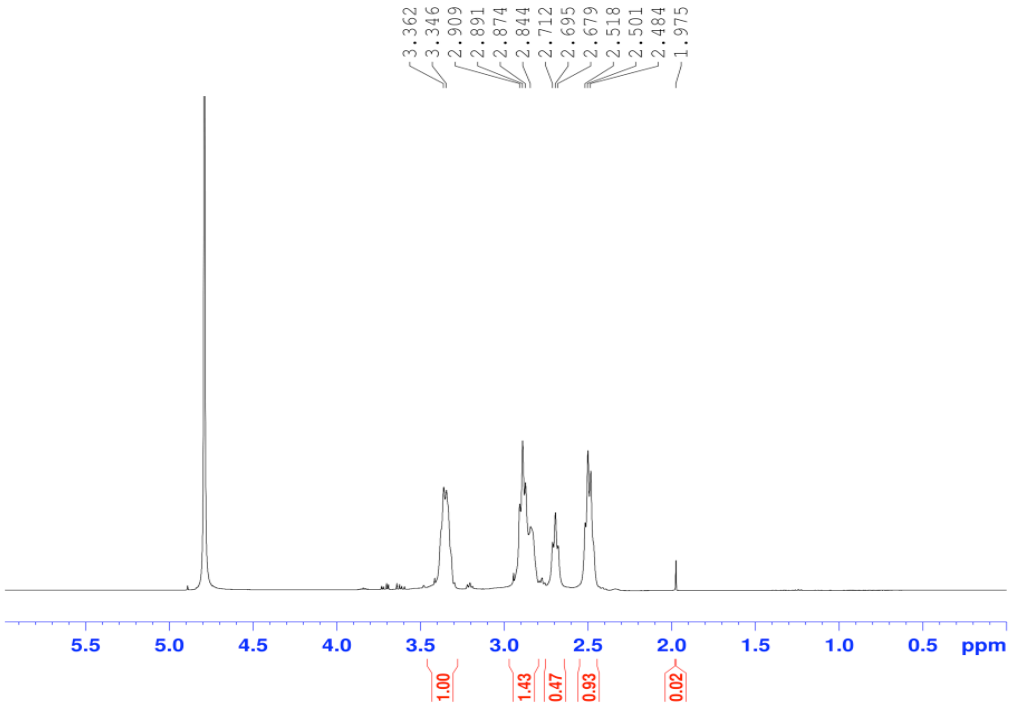

Figure 43 – ^{1}H NMR of G5 PAMAM in D_2O.

UNIVERSIDADE da MADEIRA

CQM CENTRO DE QUÍMICA DA MADEIRA

Molecular Materials RESEARCH GROUP MADEIRA ISLAND - PORTUGAL

FCT Fundação para a Ciência e a Tecnologia
MINISTÉRIO DA EDUCAÇÃO E CIÊNCIA

Governo da República Portuguesa

União Europeia

Região Autónoma da Madeira